Pricing Longevity Derivatives via Fourier Transform

Jorge M. Bravo

Universidade Nova de Lisboa - NOVA IMS

& Centro de Investigação em Gestão de Informação (MagIC)

& CEFAGE-UE & Université Paris-Dauphine PSL

E-mail: jbravo@novaims.unl.pt

João Pedro Vidal Nunes

Instituto Universitário de Lisboa (ISCTE-IUL),

Business Research Unit (BRU-IUL), Lisboa, Portugal.

E-mail: joao.nunes@iscte-iul.pt

This is the accepted author manuscript of the following article published by Elsevier:

Bravo, J. M., & Nunes, J. P. V. (2021). Pricing longevity derivatives via Fourier transforms. Insurance: Mathematics and Economics, 96(January), 81-97. [Advanced online publication on 1 November, 2020]. Doi: https://doi.org/10.1016/j.insmatheco.2020.10.008

Journal Pre-proof

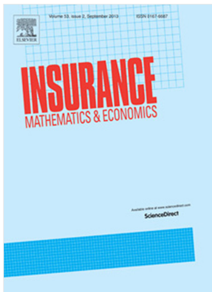

Pricing longevity derivatives via Fourier transforms

Jorge M. Bravo, João Pedro Vidal Nunes

PII: S0167-6687(20)30140-2
DOI: https://doi.org/10.1016/j.insmatheco.2020.10.008
Reference: INSUMA 2703

To appear in: *Insurance: Mathematics and Economics*

Received date : 10 March 2020
Revised date : 13 October 2020
Accepted date : 14 October 2020

Please cite this article as: J.M. Bravo and J.P.V. Nunes, Pricing longevity derivatives via Fourier transforms. *Insurance: Mathematics and Economics* (2020), doi: https://doi.org/10.1016/j.insmatheco.2020.10.008.

Pricing Longevity Derivatives via Fourier Transforms*

Jorge M. Bravo
Universidade Nova de Lisboa - NOVA IMS
& Centro de Investigação em Gestão de Informação (MagIC)
& CEFAGE-UE & Université Paris-Dauphine PSL
E-mail: jbravo@novaims.unl.pt

João Pedro Vidal Nunes†
Instituto Universitário de Lisboa (ISCTE-IUL),
Business Research Unit (BRU-IUL), Lisboa, Portugal.
E-mail: joao.nunes@iscte-iul.pt

20th October 2020

*The authors thank the anonymous referees and the editor, whose suggestions and corrections have significantly improved this article. We also thank the participants in the Fifteenth International Longevity Risk and Capital Markets Solutions Conference, Washington, September 2019. Financial support from Fundação para a Ciência e Tecnologia (FCT), grant numbers UIDB/04152/2020 and UID/GES/00315/2019, is also gratefully acknowledged by the first and second authors, respectively.

†Corresponding author. Address: ISCTE-IUL, Edifício II, Av. Prof. Aníbal Bettencourt, 1600-189 Lisboa, Portugal.

Pricing Longevity Derivatives via Fourier Transforms

Abstract

Longevity-linked derivatives are one of the most important longevity risk management solutions for pension schemes and life annuity portfolios. In this paper, we decompose several longevity derivatives—such as geared longevity bonds and longevity-spread bonds—into portfolios involving longevity options. For instance, we show that the fair value of an index-based longevity swap can be broken down into a portfolio of long and short positions in European-style longevity caplets and floorlets, with an underlying asset equal to a population-based survivor index and strike price equal to the initial preset survivor schedule. We develop a Fourier transform approach for European-style longevity option pricing under continuous-time affine jump-diffusion models for both cohort mortality intensities and interest rates, accounting for both positive and negative jumps in mortality. The model calibration approach is described and illustrative empirical results on the valuation of longevity derivatives, using U.S. total population mortality data, are provided.

JEL Code: G13, G22, C63, G12.

Keywords: Longevity Swaps; Longevity caps and floors; Longevity bonds; Affine mortality models; Fourier Transforms.

1. Introduction

Longevity increases and population ageing create challenges for all societal institutions, particularly those providing retirement income, health care, and long-term care services. Although advances in longevity are not homogenous across socioeconomic groups, securing an adequate, stable and predictable lifelong income stream and providing a cost effective and efficient risk pooling mechanism that addresses the (individual) uncertainty of death through the provision of a lifetime annuity are some of the main mechanisms pension schemes use to redistribute income in a welfare-enhancing manner—see, for instance, Ayuso et al. (2020), Sánchez-Romero et al. (2020) and Bravo and Herce (2020). Pension schemes and annuity providers face long-run solvency challenges to provide guaranteed lifetime income due to uncertain financial returns and systematic (non-diversifiable) longevity risk. The potential size of the global longevity risk market exposure for pension liabilities has been recently estimated at between $60trn and $80trn—Michaelson and Mulholland (2014).

For pension plans and annuity providers, traditional longevity risk management solutions include loss control techniques (e.g., via product re-design or risk-sharing arrangements between pensioners/policyholders and providers), natural hedging, liability selling via an insurance or reinsurance contract (through pension buy-outs, pension buy-ins or bulk annuity transfers) and insurance-based longevity swaps—D'Amato et al. (2018). Insurance-based longevity (or survivor) swaps are typically long-maturity bespoke (customized) arrangements, involving no asset transfer, by which the buyer seeking to hedge longevity risk agrees to pay a pre-agreed fixed set of cash flows to the swap (hedge) provider at predetermined future dates, in exchange for receiving a floating set of cash flows linked to the actual mortality experience of the swap buyer—see Blake et al. (2006) or Blake et al. (2019). The swap provides the pension plan a customized (i.e., with no basis risk) cash flow hedge of its longevity risk, but that comes at the expense of a higher price when compared to alternative index-based structures, reduced liquidity and lack of transparency and attractiveness to capital markets investors. Insurance-based solutions for longevity risk management are still predominant in the market despite expensive reinsurance premia and significant counterparty credit risk exposure to the hedge provider. A similar but more transparent and standardized alternative to bespoke longevity swaps are index-based capital-market longevity swaps which involve counterparties swapping fixed payments for floating payments linked to the actual survival index of a given publicly available reference population at predetermined (sequential) future calendar dates, for a given fixed notional amount. Traditional reinsurance is not a definitive answer to the problem due to the undiversifiable nature of systematic longevity risk, which cannot be eliminated by increasing the reinsurer's portfolio size and appealing to the law of large numbers. For reinsurers, the market is interesting only to the extent that the hedge provider has the chance to explore natural hedging opportunities (across lines of business or across time) or the possibility of a subsequent transfer of the risk to capital markets. The reinsurance market capacity to absorb the massive longevity risk exposure currently undertaken is limited and long-term mortality guarantees are costly since regulatory capital charges are expected to increase for providers under Solvency II framework.

As a result, in recent years several (mostly index-based) capital-market-based solutions for mortality and longevity risk management have been proposed and, some, successfully launched. They include insurance securitization, mortality- or longevity-linked securities such as CAT mortality bonds, survivor/longevity bonds (LBs)—Blake and Burrows (2001), Dowd (2003) and Cairns et al. (2008)—, longevity-spread bonds—Hunt and Blake (2015)— and derivatives with both linear and nonlinear payoff structures. The most common types of index-based mortality and longevity derivatives discussed in the literature include longevity swaps—Dowd et al. (2006)—, q-forwards—Coughlan et al. (2007)—, S-forwards—LLMA (2010)—, K-forwards—Chan et al. (2014) and Biffis et al. (2017)—, mortality options—Cairns et al. (2008)—, survivor options—Dowd (2003)—, survivor swaptions—Dawson et al. (2009)—, longevity experience options (LEO), K-options—Li et al. (2019)—and call spread options —Michaelson and Mulholland (2015) and Cairns and Boukfaoui (2019). An interesting development in the market has been the issuance of mortality- and longevity-linked structured notes incorporating derivative contracts (options), enabling coupon and/or redemption payments to depend on the performance of the underlying mortality or longevity index—see, e.g., the Swiss Re VITA I mortality bond launched in 2003, the Swiss Re longevity-spread bond (known as Kortis) issued in December 2010, or tail-risk protection instruments like the geared longevity bond (also named longevity bull call spread), negotiated by Aegon in 2012 and 2013. The incorporation of mortality and longevity options into vanilla debt structures provides hedgers of longevity risk and hedge providers a way to protect their death benefit or annuity liability risks, to limit their risk exposure (and potential profits) or to express their views on expected underlying asset developments, but requires proper valuation and risk management tools.[1]

[1]The introduction of methodologies such as MCEV and Economic Capital and recent regulatory processes (e.g., Solvency II, Swiss Solvency Test, IFRS) has led insurers to focus more closely on proper pricing and risk assessment of long-term guarantees and embedded options in life insurance.

In this paper, we focus on the valuation of index-based capital-market longevity (or survivor) options and swaps using Fourier transforms. The longevity swap can be financially engineered as a portfolio of vanilla S-forwards with predetermined (sequential) future maturity dates, whose payoff can be broken down into long and short positions in European-style (call and put) longevity options (longevity caplets and floorlets) with an underlying asset equal to a population-based survivor index and strike price equal to the initial preset (risk-adjusted) survivor schedule. The embedded auto-executable longevity options give swap counterparties the right to exchange payments based on the difference between the realized and the expected survivor-index. Blake et al. (2006) proposed engineering a longevity bond by decomposition. The pricing of longevity-linked securities via option decomposition was pioneered by Bravo and de Freitas (2018), who discuss the valuation of longevity-linked life annuities using a risk-neutral simulation approach, with longevity risk premium introduced via the Wang distortion operator. In this paper, we follow an alternative route and develop a Fourier transform approach for European-style longevity option pricing under continuous-time affine jump-diffusion models for both cohort mortality intensities and interest rates. Specifically, we assume that the mortality intensity of a given cohort is driven by an affine jump-diffusion process with "double exponential" distributed jumps, allowing for both (asymmetric) positive and negative mortality jumps of different sizes. In this setting, the risk-adjusted survival probability can be expressed in closed-form, and, hence, an analytical formula for the mark-to-market price of the S-forward can be obtained. Since the index-based longevity swap is constructed as a basket of S-forwards, the price of a longevity swap can easily be obtained as the sum of the individual S-forward prices. The affine jump-diffusion framework proposed in this paper is quite general and flexible and accommodates most short-rate and forward-rate mortality intensity models proposed in the literature.

The use of Fourier transforms for European option pricing and hedging was popularized by Carr and Madan (1999) and has been already applied in the actuarial science field—see, for instance, Chau et al. (2015) or Alonso-García and Ziveyi (2018)—but, up to our knowledge, has never been used in the valuation of longevity-linked options. We derive an analytic expression for the characteristic function of the underlying longevity index price process, obtain the Fourier transform of the damped European longevity option price and compute the corresponding Fourier inversion to recover the option price via a Gauss-Lobatto quadrature scheme.

In order to price longevity-linked securities, the underlying stochastic mortality rate process needs to be specified under a risk-neutral (equivalent-martingale) probability measure. Following Cairns et al. (2006b), we use a risk-neutral valuation approach to incorporate the market price of longevity risk. Although longevity derivatives are still traded in an incomplete market setting and it is not possible to replicate the payoffs of the contract dynamically and to infer risk-neutral probabilities from market transaction data, the use of a risk-neutral pricing measure guarantees that different longevity-linked securities are priced consistently.[2] We provide illustrative empirical results on the pricing of longevity swaps (of different tenors) using U. S. mortality data from 1960 to 2017 for representative cohorts.

In the literature, several continuous-time stochastic mortality models have been proposed for modelling the dynamics of mortality rates—see, for example, Milevsky and Promislow (2001), Dahl (2004), Biffis (2005), Cairns et al. (2006a,b, 2008), Biffis and Millossovich (2006), Schräger (2006), Miltersen and Persson (2006), Ballotta and Haberman (2006), Luciano and Vigna (2008), Bravo (2007, 2011), Zhu and Bauer (2011), Luciano et al. (2012), Fung et al. (2019) and references therein.[3] The task of modelling (and managing) longevity risk is challenging since the nature of the risk addressed is multivariate, encompassing mortality trend uncertainty, longevity diffusion risk, mortality jump risk, as well as model and parameter risk. Cox et al. (2006) argue that an appropriate stochastic mortality model should incorporate mortality jumps since the rationale for trading mortality-linked securities is to hedge or take (in some cases catastrophic) mortality or longevity risks. The authors propose a one-time jump-diffusion model to describe mortality rate dynamics, combining a Brownian motion and a single compound Poisson process for mortality jumps. Chang et al. (2010) extend the model by considering mortality jumps and default risk simultaneously, and use it to price vanilla survivor swaps. Luciano and Vigna (2008) investigate the empirical performance of several single factor mean-reverting and non-mean reverting stochastic

[2]The pricing of longevity-linked securities using risk-neutral valuation can always be compared with that obtained using alternative approaches proposed to approximate the prices of longevity-linked securities in an incomplete market setting, namely the Wang transform—Wang (2002)—, the instantaneous Sharpe ratio method—Milevsky et al. (2005)—, the Equivalent Utility Pricing Principle—Cui (2008)—, the Cost of Capital approach—Levantesi and Menzietti (2006) and Zeddouk and Devolder (2019)—, multivariate exponential tilting—Cox et al. (2006)—or the CAPM- (and CCAPM-) based approaches—Friedberg and Webb (2005).

[3]Bravo et al. (2020) propose an alternative novel approach based on an adaptive Bayesian Model Ensemble (model combination) of heterogeneous stochastic mortality models, all of which can probabilistically contribute towards projecting future mortality rates.

mortality models (some including a single jump component) using UK cohort population data, and conclude that non-mean reverting processes with a deterministic part that increases exponentially seem to be appropriate to capture the dynamics of human mortality with age. Typically, catastrophic mortality events have very low frequency, their occurrence has the potential to severely affect human mortality, but its impact vanishes quickly with time. Lin et al. (2010) propose a stochastic mortality model featuring both a trend reduction jump component (to describe permanent longevity improvements) and a temporary mortality jump process (to capture severe but transitory effects on death rates), along with a general longevity trend, modelled using the classical age-period Lee and Carter (1992) model. Their model also captures the asymmetrical effect of mortality events on different ages. Li and Liu (2015) introduce a Lee–Carter variant that captures the age pattern of mortality jumps.

In this paper, we extend previous research and propose, as our "baseline model", a non-mean reverting square-root jump diffusion Feller process combined with a Poisson process with double asymmetric exponentially distributed jumps—Kou and Wang (2004)—to account for both negative (e.g., new rare medical breakthroughs resulting in sudden improvements in mortality, healthier life styles that reduce important causes of death) and positive jumps (e.g., wars, pandemics or natural disasters resulting in abrupt catastrophic episodes in mortality) of different sizes. Previous research considering jump processes in stochastic mortality modelling focused almost exclusively on the impact of negative mortality jumps to describe longevity risk. Although long term mortality trends suggest that unexpected survival gains dominate catastrophic mortality episodes, we believe a rich and flexible mortality approach should encompass both mortality improvement and deterioration jump factors. The deterministic part of the model increases exponentially with age, as observed at adult ages in most countries, and follows the Gompertz law in expected terms. The square-root jump diffusion component guarantees positive mortality rates. The model is parsimonious, offers analytical tractability, and has proven to fit accurately both historical and projected mortality data—Luciano and Vigna (2008) and Bravo (2007)—, fulfilling the requirements for a good mortality model listed by Cairns et al. (2006a). Compared to alternative approaches (for example, Monte Carlo simulation methods), the model allows for closed-form expressions for longevity option prices and longevity-linked structured securities, permitting efficient computation of prices and sensitivity measures (i.e., risk statistics or Greeks) that are required to perform dynamic hedging.

The valuation of longevity-linked derivatives with non-linear payoff structures (e.g., longevity options) has received little attention in the literature compared to that of longevity derivatives with a linear payoff but is attracting increasing interest. Some exceptions are Lin and Cox (2007), who study the pricing of a longevity call option linked to a population longevity index for older ages, Cui (2008), who discusses the valuation of longevity options (floors and caps) using the Equivalent Utility Pricing Principle, Dawson et al. (2010), who derive closed-form Black-Scholes-Merton-type prices for European swaptions, Boyer and Stentoft (2013), who price European and American type survivor options using a risk neutral simulation approach, Wang and Yang (2013), who price survivor floors using an extension of the Lee-Carter model, Yueh et al. (2016), who develop valuation models for mortality calls and puts—employing the jump-diffusion model developed by Cox et al. (2006)—, Bravo and de Freitas (2018) and Bravo (2019, 2020), who discuss the valuation of longevity options embedded in longevity-linked life annuities, Fung et al. (2019), who derive closed-form solutions for the price of longevity caps under a two-factor Gaussian mortality model resembling the Black-Scholes formula for option pricing when the underlying stock price follows a geometric Brownian motion, and Li et al. (2019) as well as Cairns and Boukfaoui (2019), who discuss the valuation of K-options and call-spreads, respectively.

This paper contributes to the literature by first using a Fourier transform approach for longevity option pricing under continuous-time affine jump-diffusion models for both cohort mortality intensities and interest rates. We derive an analytic expression for the characteristic function of the underlying asset price process, define the optimal integration contour and dampening parameter, and recover the longevity option price via a Gaussian quadrature. Second, geared longevity bonds, longevity-spread bonds, and index-based survivor swaps are decomposed into portfolios of long and short positions in European-style (call and put) longevity options, which form the building blocks from which other more complex longevity-linked securities and derivatives can be constructed and priced.[4] Third, we develop a tractable and biologically reasonable continuous time affine jump-diffusion stochastic mortality model, considering for both positive and negative mortality jumps with sizes following a double asymmetric exponential distribution. The analytical tractability of the model allows

[4] In opposition, previous research on, for instance, the marking to market and hedging of survivor swaps typically follows a traditional valuation approach based on the discounted difference between the realized survival probability and some preset survival rate—see, e.g., Dowd et al. (2006), Lin and Cox (2005), Dahl et al. (2008), Chang et al. (2010), Dawson et al. (2010), Dahl et al. (2011), Boyer and Stentoft (2013), Zeddouk and Devolder (2019) and Fung et al. (2019).

us to derive closed-form solutions for the survival probability and quasi-explicit analytical solutions for the price of option-type longevity derivatives (longevity caplets and floorlets, S-forwards and longevity swaps). Finally, we successfully calibrate the model to U.S. mortality data and present illustrative longevity swap valuation results.

The remainder of the paper is organized as follows. Section 2 presents the general framework for the valuation of longevity derivatives with different payoff structures, using a Fourier transform approach. The analysis covers option-type contracts (longevity caps and floors), S-forwards and longevity swaps. Section 3 develops the analytical pricing model for longevity derivatives under a risk-adjusted probability pricing measure, and comprises: the description of the continuous-time affine jump-diffusion stochastic process proposed for both the mortality intensity and interest rates, the derivation of an analytical expression for the relevant characteristic function, and the estimation of the optimal dampening parameter. Section 4 describes the model calibration approach and provides illustrative empirical results on the valuation of longevity derivatives using U.S. total population mortality data. Finally, Section 5 concludes. All accessory results are relegated to a supplementary file available at http://home.iscte-iul.pt/~jpvn/weblinks/SFIME20.pdf.

2. Valuation of longevity derivatives using Fourier transforms

In this section, we present the general framework for the valuation of longevity derivatives with different payoff structures, using a Fourier transform approach. The analysis covers option-type contracts (longevity caplets and floorlets), geared longevity bonds, longevity-spread bonds, S-forwards and longevity swaps.

Hereafter, let τ_x denote a non-negative random variable representing the residual lifetime of an individual aged x at present time $t = 0$. Following, e.g., Biffis (2005), Schräger (2006) and Biffis et al. (2010), we consider the time interval $[0, \omega]$, with ω denoting the highest attainable age, and define the stochastic force of mortality process on a filtered probability space $(\Omega, \mathbb{G}, \mathbb{P})$ with filtration $\mathbb{G} = (\mathcal{G}_t)_{t\in[0,\omega-x]}$ ($\mathcal{G}_0 = \{\emptyset, \Omega\}$) and $\mathbb{P}$ denoting the real world probability measure. More precisely, filtration $\mathbb{G}$ contains two strict subfiltrations $\mathbb{D}$ and $\mathbb{H}$. $\mathbb{D} = (\mathcal{D}_t)_{t\in[0,\omega-x]}$, with σ-algebra $\mathcal{D}_t = \sigma\left(\mathbf{1}_{\{\tau_x\leq s\}} : 0 \leq s \leq t\right)$, denotes the minimal sub-filtration needed to generate τ_x as the first jump-time of a nonexplosive $\mathbb{G}$-counting process

$\left(\mathbf{1}_{\{\tau_x \leq s\}}\right)_{t\geq 0}$, recording at each time $t \geq 0$ whether the individual has died or survived. The stopping time τ_x is said to admit an intensity μ_x if the compensator of the counting process does. The subfiltration $\mathbb{H} = (\mathcal{H}_t)_{t\in[0,\omega-x]}$ describes all information except whether the person is alive up to time t, including information about the dynamics of the mortality intensity. Under this setting, the remaining lifetime of an individual is a doubly stochastic stopping time with intensity μ_x. Hereafter, $\mathcal{G}_t = \mathcal{D}_t \vee \mathcal{H}_t$, with $\mathcal{H}_t = \mathcal{M}_t \vee \mathcal{F}_t$, and where $\mathcal{M}_t$ and $\mathcal{F}_t$ contain the information concerning mortality and financial markets, respectively.

2.1. Engineering longevity-linked securities using longevity options

One of the possible ways to construct a longevity-linked security is by decomposing and financially engineering its cash flows combining conventional bonds, forward contracts, longevity swaps and longevity options. For instance, Blake et al. (2006) discuss how to engineer a longevity bond combining longevity zeros (LZ) and a longevity swap, or combining LZs with a series of forward contracts, or combining a conventional bond with an option that hedges the tail risk. A second example are the so-called geared longevity bonds (or longevity bull call spreads) designed to deliver tail-risk protection and discussed in Blake et al. (2006) and Blake et al. (2019). The bonds have payments contingent on the reference population survival index $S(x,t)$ and make payments to the hedger provided that the underlying asset is observed within a predetermined narrower band (corridor), say if $S(x,t) \in [S_l(t), S_u(t)]$, where $S_l(t)$ and $S_u(t)$ denote attachment and exhaustion points, respectively, defined such that the hedge is out-of-money at inception. The survival index, attachment point, and exhaustion point determine whether the bond is triggered and if so, the maximum bond payoff. The bond payoff at time t can be decomposed as

$$\begin{aligned} C(t) &= \mathbb{1}_{\{0<S(x,t)<S_l(t)\}} \times 0 + \mathbb{1}_{\{S_l(t)\leq S(x,t)\leq S_u(t)\}} \left(S(x,t) - S_l(t)\right) \\ &\quad + \mathbb{1}_{\{S(x,t)>S_u(t)\}} \left(S_u(t) - S_l(t)\right) \\ &= \min\left[S_u(t) - S_l(t); \max\left(S(x,t) - S_l(t), 0\right)\right], \end{aligned} \tag{1}$$

or, equivalently, as

$$C(t) = \left(S(x,t) - S_l(t)\right) + \left(S_l(t) - S(x,t)\right)^+ - \left(S(x,t) - S_u(t)\right)^+, \tag{2}$$

where $a^+ := \max(a, 0)$.

From equation (2) we observe that the payoff at time t can be financially engineered combining a long position in a forward contract, a long position in a longevity floorlet on $S(x,t)$ with strike price $S_l(t)$ and a short position in a longevity caplet on $S(x,t)$ with a strike price $S_u(t)$. In the option terminology, the payoff in equation (2) resembles that of a long "bull call spread". By setting $S_l(t)$ and $S_u(t)$ such that the value of the longevity floorlet and the longevity caplet are equal, the geared longevity bond payoff resumes to that of a portfolio comprising a long position in a longevity bond paying $S(x,t)$ periodically and a short position in a fixed rate bond paying $S_l(t)$.

A third example is the longevity-spread bond (Kortis bond) discussed in Hunt and Blake (2015). The bond pays quarterly coupons at LIBOR + 5.0% but the redemption of principal at maturity is at risk and contingent on a longevity divergence index value (LDIV) measuring the divergence in mortality rates between the male populations in England & Wales (EW) and the United States (US). The LDIV, $\mathcal{L}_t^{DIV}$, is calculated for year t as

$$\mathcal{L}_t^{DIV} = \mathcal{I}_t^{EW} - \mathcal{I}_t^{US}, \tag{3}$$

where $\mathcal{I}_t^p$ denotes, in population $p \in \{EW, US\}$, the average improvement in mortality rates observed across the range of ages considered in the eight years of the bond. The reduction of the principal amount of the Kortis bond is triggered if the $\mathcal{L}_t^{DIV}$ value exceeds the attachment point (AP) by a "principal reduction factor" (PRF) given by

$$PRF(t) = \max\left(\min\left(\frac{\mathcal{L}_t^{DIV} - AP}{EP - AP}, 1\right), 0\right), \tag{4}$$

with $AP = 3.4\%$, while $EP = 3.9\%$ represents the exhaustion point.[5] Equation (4) shows that the bond was structured such that once the attachment point is exceeded, the reduction in the principal amount increases linearly (between the attachment and exhaustion points) until the divergence index exceeds the exhaustion point and the full principal is lost by the bondholder. The PRF at time t can be rewritten as

$$PRF(t) = \frac{1}{EP - AP}\left[\left(\mathcal{L}_t^{DIV} - AP\right) + \left(AP - \mathcal{L}_t^{DIV}\right)^+ - \left(\mathcal{L}_t^{DIV} - EP\right)^+\right], \tag{5}$$

and resembles again the payoff of a long "bull call spread" on $\mathcal{L}_t^{DIV}$, i.e., it can be financially engineered—up to a constant multiple $1/(EP - AP)$—combining a long position in a forward contract on $\mathcal{L}_t^{DIV}$ with forward rate AP, a long position in a put option on the longevity divergence index with strike price AP, and a short position in a call option on $\mathcal{L}_t^{DIV}$ with a strike price EP.

[5] A similar payoff function can be found in call spread options—see, e.g., Cairns and Boukfaoui (2019).

A fourth example of financially engineering a mortality or longevity-linked security using options is the Swiss Re mortality bond (Vita I) issued in 2003. The bond paid quarterly coupons set at three-month U.S. dollar LIBOR+135 basis points but the principal was at risk and contingent on what happened to a composite index q_t constructed as a weighted average of mortality rates over age and sex of five countries (US, UK, France, Italy, and Switzerland). It can be shown that the principal payoff of the Swiss Re Bond can be written as that of an Asian-type put option on the difference between q_t and an attachment point (1.3 times the base level q_0) with strike price equal to q_0. The principal would be completely exhausted if the index exceeds 1.5 times the base level. A fifth example is the "longevity experience option" introduced by Deutsche Bank in November 2013. The contract is structured as an out-of-the-money call option spread on 10-year forward survival rates of the male and female populations of England & Wales and the Netherlands derived from LLMA longevity indices in five-year age cohorts (between 50 to 79).

A sixth example is the longevity-linked life annuities (LLLA) discussed in Bravo and de Freitas (2018). The distinguishing feature of this contract is that the annuity benefit is linked to a longevity index $\mathcal{I}_{t_0+k}$ expressing the ratio between the best-estimate and the actual probability of a given cohort aged x_0 at time t_0 to survive to age x_0+k, $k=1,...,\omega-x_0$. The authors show that LLLAs can be decomposed into conventional life annuities and baskets of European-style longevity (call and put) options of different maturities with underlying asset equal to $\mathcal{I}_{t_0+k}$ with, for capped contract, some upper and lower barriers. For instance, for capped LLLAs, annuity payments b_{t_0+k} can be expressed as a protective longevity collar, i.e., a combination between the underlying, a long position in a longevity floorlet with strike $\mathcal{I}^{\min}_{t_0+k}$ and a short position in a longevity caplet with strike $\mathcal{I}^{\max}_{t_0+k}$:

$$b_{t_0+k} = \mathcal{I}_{t_0+k} + \left(\mathcal{I}^{\min}_{t_0+k} - \mathcal{I}_{t_0+k}\right)^+ - \left(\mathcal{I}_{t_0+k} - \mathcal{I}^{\max}_{t_0+k}\right)^+ . \tag{6}$$

Alternatively, the annuity payoff can be represented by a long position in a longevity caplet spread or by a short position in a longevity floorlet spread.[6]

Finally, this paper also shows—in Subsection 2.4—that the fair value of index longevity swaps can be engineered by a portfolio comprising a long position in longevity caplets and a short position in longevity floorlets with underlying equal to the actual survival probability and strike price given by the preset risk-adjusted survivor schedule. Before that, we present the building blocks from which any more complex longevity-linked security can be structured and priced.

[6] Please, see Bravo and de Freitas (2018) for details.

2.2. First building block: longevity caplets

A longevity cap is an option-type longevity-linked derivative instrument by which the buyer receives payments at the end of each contractual period if the survival rate in a reference population cohort exceeds the strike price agreed at the inception of the contract. Similarly to an interest rate cap, the longevity cap can be broken down into a series of sequentially maturing European-style call options (longevity caplets) with common underlying asset and a preset strike price. Hence, the fair value of a longevity cap is the sum of these longevity caplet prices.

To price a longevity caplet, let ${}_{T}p_{x}^{obs}(T)$ denote the T-year (observed) realized survival rate of a reference population cohort aged x at time 0:

$$ {}_{T}p_{x}^{obs}(T) := \exp\left(-\int_{0}^{T} \mu_{x+s}(s)\, ds\right), \tag{7} $$

where $\mu_{x+s}(s)$ is the mortality intensity of an individual aged $x+s$ at time s.[7] The terminal payoff of a longevity caplet on the realized survival rate ${}_{T}p_{x}^{obs}(T)$, maturing at time T, with fixed strike $K \in \mathbb{R}_{+}$ and notional amount equal to one monetary unit is equal to

$$ c_{T}\left({}_{T}p_{x}^{obs}(T), K, T\right) = \left[\exp\left(-\int_{0}^{T} \mu_{x+s}(s)\, ds\right) - K\right]^{+}. \tag{8} $$

The strike can be stated as some percentage of the T-year (real world) survival probability of a cohort aged x at time 0 ($\mathcal{G}_0$ measurable), i.e.

$$ K = \kappa \times {}_{T}p_{x}(0)\,, \tag{9} $$

for $\kappa \in \mathbb{R}_{+}$. For instance, if the insurer (seller of longevity risk protection) demands a positive market price of longevity risk premium, the risk-adjusted survival probability will be larger than the "best estimate" $\mathbb{P}$-survival probability, and, hence, $\kappa > 1$ for an at-the-money option. The goal is to find the time-0 price for this contract, i.e.

$$ \begin{aligned} & c_{0}\left({}_{T}p_{x}^{obs}(T), K, T\right) \\ = \ & \mathbb{E}_{\mathbb{Q}}\left\{ \exp\left(-\int_{0}^{T} r_s ds\right) \times \left[\exp\left(-\int_{0}^{T} \mu_{x+s}(s)\, ds\right) - \kappa \times {}_{T}p_{x}(0)\right]^{+} \middle| \mathcal{G}_0 \right\} \\ = \ & \mathbb{E}_{\mathbb{Q}}\left\{ \exp\left(-\int_{0}^{T} r_s ds\right) \times \left[\exp\left(-\int_{0}^{T} \mu_{x+s}(s)\, ds\right) - \kappa \times {}_{T}p_{x}(0)\right]^{+} \middle| \mathcal{H}_0 \right\}, \end{aligned} \tag{10} $$

[7] Note that the mortality model follows a single cohort throughout time, which means that the forecasted mortality intensity at future (older) ages (and calendar years) includes both an age effect and a period effect.

where $\{r_t : t \geq 0\}$ is the risk-free instantaneous interest rate process, $\mathbb{Q}$ is the equivalent martingale measure that takes the "money-market account" as numeraire, and it is assumed that $\tau_x > 0$.

Changing the numeraire from the "money-market account" to the zero-coupon risk-free bond with maturity at time T—and time-0 price $P(0,T)$—that is associated to the equivalent forward measure $\mathbb{Q}_T$, then equation (10) can be restated as

$$c_0\left({}_T p_x^{obs}(T), K, T\right) = P(0,T)\,\mathbb{E}_{\mathbb{Q}_T}\left\{\left[\exp\left(-\int_0^T \mu_{x+s}(s)\,ds\right) - \kappa \times {}_T p_x(0)\right]^+ \middle| \mathcal{H}_0\right\}. \tag{11}$$

Since ${}_T p_x^{obs}(T)$ only takes values in $]0,1[$, it is not possible to define the Fourier transform of the expectation contained on the right-hand side of equation (11) with respect to the strike. For this purpose, the option value can be rewritten as

$$c_0\left({}_T p_x^{obs}(T), K, T\right) = P(0,T)\,{}_T p_x(0)\,\mathbb{E}_{\mathbb{Q}_T}\left\{\left[I_x(0,T) - \kappa\right]^+ \middle| \mathcal{H}_0\right\}, \tag{12}$$

where

$$I_x(0,T) := \frac{\exp\left(-\int_0^T \mu_{x+s}(s)\,ds\right)}{{}_T p_x(0)} \tag{13}$$

is a longevity index defined as the ratio between the observed and the expected T-year survival probability of a cohort aged x at time 0. The longevity index takes values in $\mathbb{R}_+$ since ${}_T p_x^{obs}(T), {}_T p_x(0) \in\ ]0,1[$. The term $P(0,T)\,{}_T p_x(0)$ denotes the usual actuarial discount factor taking both the survival probability and the time value of money into account. Moreover, and since both $I_x(0,T)$ and κ take values in $\mathbb{R}_+$, their logs will lie over the entire real line, and equation (12) becomes

$$c_0\left({}_T p_x^{obs}(T), K, T\right) = P(0,T)\,{}_T p_x(0)\,V(0,T;\omega), \tag{14}$$

where

$$V(0,T;\varpi) := \mathbb{E}_{\mathbb{Q}_T}\left\{\left[e^{z_x(0,T)} - e^{\varpi}\right]^+ \middle| \mathcal{H}_0\right\}, \tag{15}$$

with

$$z_x(0,T) := \ln I_x(0,T), \tag{16}$$

and

$$\varpi := \ln \kappa. \tag{17}$$

Following Carr and Madan (1999) and Lee (2004), next proposition offers a quasi-explicit solution for the expectation (15) in terms of the characteristic function of the log longevity index, which is defined as

$$g\left(t,T;\phi;\mu_{x+t}\left(t\right)\right):=\mathbb{E}_{\mathbb{Q}_T}\left[\left.e^{i\phi z_x(t,T)}\right|\mathcal{H}_t\right], \tag{18}$$

for $\phi\in\mathbb{C}$.

Proposition 1 *The time-*0 *fair value of the longevity caplet with terminal payoff (8) is given by equation (14) with*

$$\begin{aligned}&V\left(0,T;\varpi\right) \\ =\;& R\left(\alpha\right)+\frac{e^{\varpi}}{\pi}\int_{0-i(\alpha+1)}^{\infty-i(\alpha+1)}\operatorname{Re}\left[e^{-iz\varpi}\varsigma\left(0,T;z+i\left(\alpha+1\right);\alpha\right)\right]dz,\end{aligned} \tag{19}$$

where ϖ *is defined by equation (17),* α *is any real number such that*

$$g\left(0,T;-i\left(1+\alpha\right);\mu_x\left(0\right)\right)<\infty,$$

$$\varsigma\left(0,T;u;\alpha\right):=\frac{g\left(0,T;u-i\left(1+\alpha\right);\mu_x\left(0\right)\right)}{\left(\alpha+iu\right)\left(\alpha+1+iu\right)}, \tag{20}$$

for $u\in\mathbb{R}$*, and*

$$R\left(\alpha\right):=\begin{cases} g\left(0,T;-i;\mu_x\left(0\right)\right)-e^{\varpi}\Longleftarrow\alpha<-1\\ g\left(0,T;-i;\mu_x\left(0\right)\right)-\frac{1}{2}e^{\varpi}\Longleftarrow\alpha=-1\\ g\left(0,T;-i;\mu_x\left(0\right)\right)\Longleftarrow-1<\alpha<0\\ \frac{1}{2}g\left(0,T;-i;\mu_x\left(0\right)\right)\Longleftarrow\alpha=0\\ 0\Longleftarrow\alpha>0\end{cases}. \tag{21}$$

Proof. Using the notation in Lee (2004), Proposition 1 follows from Lee (2004, Theorem 5.1) when the payoff function G_1 is considered and the (discounted) characteristic function $f\left(z\right)$ is replaced by $g\left(0,T;z;\mu_x\left(0\right)\right)$. For more details, please see Section A of the supplementary file. ∎

The integral contained on the right-hand side of equation (19) will be computed using a Gauss-Lobatto integration rule that is implemented through *Matlab* (R2017a) running on an Intel Xeon 3.33 GHz processor with 12GB of RAM memory. For this purpose, and after applying the change of variables $z=u-i\left(\alpha+1\right)$, the integral boundaries $[0,\infty)$ of equation

(19) are then mapped into the closed interval $[0,1]$ through a transformation similar to the one proposed by Kahl and Jäckel (2005, Equation 41)—i.e. $u = -\ln x$—, yielding

$$V(0,T;\varpi) = R(\alpha) + \frac{e^{\varpi-(\alpha+1)\varpi}}{\pi}\int_0^\infty \mathrm{Re}\left[e^{-iu\varpi}\varsigma(0,T;u;\alpha)\right]du \tag{22}$$

$$= R(\alpha) + \frac{e^{-\alpha\varpi}}{\pi}\int_0^1 \mathrm{Re}\left[x^{i\varpi}\varsigma(0,T;-\ln x;\alpha)\right]dx. \tag{23}$$

The Gauss-Lobatto integration rule employed—implemented with machine precision, and based on the adaptive scheme proposed by Gander and Gautschi (2000)—is shown by Nunes and Alcaria (2016) to offer the best speed-accuracy trade-off amongst different Gaussian quadrature and discrete Fourier transform integration methods. Note, however, that the integrand of equation (22) is not defined in *Matlab* for extremely large abscissas, even though it vanishes at infinity. Therefore, the integral on the right-hand side of equation (23) is computed not in the closed interval $[0,1]$ but rather on $[10^{-16},1]$. Nevertheless, the associated truncation error is found to be negligible: the same numerical results follow when computing the integral on the right-hand side of equation (22) via discrete Fourier transform integration, using a log-strike grid comprising 16,384 prices (centered around ϖ), with a constant spacing of size 0.01, and through the Davis (1973) style (midpoint) sampling scheme proposed by Lee (2004, Equation 6.1 and Appendix C).

2.3. Second building block: longevity floorlets

Consider now a longevity floor, an option-type longevity-linked derivative by which the buyer receives payments at the end of each contractual period if the survival rate in a reference population cohort is below the strike price agreed at contract inception. Similarly to an interest rate floor, the longevity floor can be decomposed into a series of sequentially maturing European put options (longevity floorlets) with common underlying asset and strike. Therefore, the fair value of a longevity floor is the sum of these longevity floorlet prices.

The terminal payoff of a longevity floorlet on the realized survival rate ${}_Tp_x^{obs}(T)$, with maturity at time T, fixed strike $K \in \mathbb{R}_+$ and notional amount equal to one monetary unit is

$$p_T\left({}_Tp_x^{obs}(T), K, T\right) = \left[K - \exp\left(-\int_0^T \mu_{x+s}(s)\,ds\right)\right]^+, \tag{24}$$

where the strike is defined as in equation (9).

Assuming that $\tau_x > 0$, the time-0 value of this contract is

$$\begin{aligned} & p_0\left({}_Tp_x^{obs}(T), K, T\right) \\ = \; & \mathbb{E}_{\mathbb{Q}}\left\{\exp\left(-\int_0^T r_s ds\right) \times \left[\kappa \times {}_Tp_x(0) - \exp\left(-\int_0^T \mu_{x+s}(s)\, ds\right)\right]^+ \middle| \mathcal{H}_0\right\} \\ = \; & P(0,T)\,\mathbb{E}_{\mathbb{Q}_T}\left\{\left[\kappa \times {}_Tp_x(0) - \exp\left(-\int_0^T \mu_{x+s}(s)\, ds\right)\right]^+ \middle| \mathcal{H}_0\right\}, \end{aligned} \tag{25}$$

where the last line arises from the change of measure $\mathbb{Q}$ to $\mathbb{Q}_T$.

Similarly to equation (12), the option value can be rewritten as

$$p_0\left({}_Tp_x^{obs}(T), K, T\right) = P(0,T)\, {}_Tp_x(0)\, \mathbb{E}_{\mathbb{Q}_T}\left\{\left[\kappa - I_x(0,T)\right]^+ \middle| \mathcal{H}_0\right\}, \tag{26}$$

where the longevity index $I_x(0,T)$ is still defined through equation (13). Therefore, and using equations (16) and (17), equation (26) can be restated as

$$p_0\left({}_Tp_x^{obs}(T), K, T\right) = P(0,T)\, {}_Tp_x(0)\, U(0,T;\omega), \tag{27}$$

where

$$U(0,T;\varpi) := \mathbb{E}_{\mathbb{Q}_T}\left\{\left[e^{\varpi} - e^{z_x(0,T)}\right]^+ \middle| \mathcal{H}_0\right\} \tag{28}$$

is given by the following proposition.

Proposition 2 *The time-*0 *fair value of the longevity floorlet with terminal payoff (24) is given by equation (27) with*

$$U(0,T;\varpi) = V(0,T;\varpi) - g(0,T;-i;\mu_x(0)) + e^{\varpi}, \tag{29}$$

where ϖ is defined by equation (17), and $g(\cdot)$ is the characteristic function (18).

Proof. Using equations (15) and (28), then

$$\begin{aligned} & V(0,T;\varpi) - U(0,T;\varpi) \\ = \; & \mathbb{E}_{\mathbb{Q}_T}\left\{\left[e^{z_x(0,T)} - e^{\varpi}\right]^+ \middle| \mathcal{H}_0\right\} - \mathbb{E}_{\mathbb{Q}_T}\left\{\left[e^{\varpi} - e^{z_x(0,T)}\right]^+ \middle| \mathcal{H}_0\right\} \\ = \; & \mathbb{E}_{\mathbb{Q}_T}\left[e^{z_x(0,T)} - e^{\varpi} \middle| \mathcal{H}_0\right] \\ = \; & g(0,T;-i;\mu_x(0)) - e^{\varpi}, \end{aligned}$$

where the last line follows from definition (18) and yields equation (29). ■

2.4. Longevity Swaps

An index-based capital-market longevity (or survivor) swap involves counterparties swapping fixed payments (fixed leg) for payments linked to the actual survival rate of a given reference population cohort (floating leg) at predetermined (sequential) future calendar dates $t_1 < t_2 < ... < t_n$, and for a given fixed notional amount N. Longevity swaps can be regarded as a portfolio of sequentially maturing survivor forwards (or S-forwards) with common notional amount and underlying asset. Compared to, e.g., longevity bonds, longevity swaps offer a cheaper longevity risk hedging solution since they do not require initial capital disbursement at contract inception.

At predetermined future calendar dates t_k $(k = 1, 2, ..., n)$, the hedger pays ${}_{t_k}p_x(0) \times N$ (fixed leg) and in exchange receives ${}_{t_k}p_x^{obs}(t_k) \times N$ (floating leg). Hence, and using definition (7), the time-t_k payoff of the longevity swap, on the kth reset date, is

$$F^S(t_k) := N \times \left[\exp\left(-\int_0^{t_k} \mu_{x+s}(s)\, ds\right) - {}_{t_k}p_x(0)\right], \tag{30}$$

which corresponds to the (terminal) payoff of a S-forward contract maturing at time t_k.

Assuming that $\tau_x > 0$, the time-0 value of the longevity swap is equal to

$$V_0 = \mathbb{E}_{\mathbb{Q}}\left[\sum_{k=1}^{n} \exp\left(-\int_0^{t_k} r_s ds\right) F^S(t_k) \middle| \mathcal{H}_0\right] \tag{31}$$

$$= \mathbb{E}_{\mathbb{Q}}\left\{\sum_{k=1}^{n} \exp\left(-\int_0^{t_k} r_s ds\right) N \left[\exp\left(-\int_0^{t_k} \mu_{x+s}(s)\, ds\right) - {}_{t_k}p_x(0)\right] \middle| \mathcal{H}_0\right\}. \tag{32}$$

Next proposition provides a closed-form solution for index-based longevity swaps and is based on the traditional pricing approach, as proposed, for instance, in Dowd et al. (2006), but under a Fourier transform setting.

Proposition 3 *The time-0 fair value of the longevity swap with time-t_k payoff (30) is equal to*

$$V_0 = N \times \sum_{k=1}^{n} P(0, t_k) \times {}_{t_k}p_x(0) \times [g(0, t_k; -i; \mu_x(0)) - 1], \tag{33}$$

where $g(\cdot)$ is the characteristic function (18).

Proof. Using equation (32), and changing from measure $\mathbb{Q}$ to the forward measure $\mathbb{Q}_{t_k}$, then

$$V_0 = N \times \sum_{k=1}^{n} P(0, t_k) \times \left\{\mathbb{E}_{\mathbb{Q}_{t_k}}\left[\exp\left(-\int_0^{t_k} \mu_{x+s}(s)\, ds\right) \middle| \mathcal{H}_0\right] - {}_{t_k}p_x(0)\right\}, \tag{34}$$

because ${}_{t_k}p_x(0)$ is $\mathcal{H}_0$-measurable.

Moreover, equations (13), (16) and (18) imply that

$$\begin{aligned} g(0,t_k;-i;\mu_x(0)) &= \mathbb{E}_{\mathbb{Q}_{t_k}}\left[e^{z_x(0,t_k)} \middle| \mathcal{H}_0 \right] \\ &= \mathbb{E}_{\mathbb{Q}_{t_k}}\left[I_x(0,t_k) \middle| \mathcal{H}_0 \right] \\ &= \frac{\mathbb{E}_{\mathbb{Q}_{t_k}}\left[\exp\left(-\int_0^{t_k} \mu_{x+s}(s)\,ds \right) \middle| \mathcal{H}_0 \right]}{{}_{t_k}p_x(0)}. \end{aligned} \tag{35}$$

Therefore, equation (33) arises after combining equations (34) and (35). ■

Alternatively, and following the longevity option decomposition approach developed by Bravo and de Freitas (2018) for the valuation of longevity-linked securities, the fair value of a fixed-rate payer longevity swap can be engineered as a portfolio of long positions in vanilla S-forwards with predetermined (sequential) future maturity dates. The terminal payoff of each S-forward is equivalent to a portfolio comprising a long position in a European-style longevity caplet (call option) and a short position in a European-style longevity floorlet (put option), with an underlying asset equal to the realized survival probability and strike price equal to the preset risk-adjusted survivor schedule. Recall that, by construction, the put-call parity requires a close relationship between European-style option prices and the forward contract premium maturing at the same time as the options. In the current example, a portfolio comprising a long position in a longevity caplet and a short position in a longevity floorlet (with the same maturity) has a value equal to the present value of a fixed leg payer in a S-forward contract maturing at the same time as the options. Therefore, and combining equations (9), (14), (27) and (29), it follows that

Remark 1 *The time-0 fair value (33) of the longevity swap with time-t_k payoff (30) can also be written as*

$$\begin{aligned} V_0 &= N \times \sum_{k=1}^{n} P(0,t_k) \times {}_{t_k}p_x(0) \times [V(0,T;0) - U(0,T;0)] \\ &= N \times \sum_{k=1}^{n} \left[c_0\left({}_{t_k}p_x^{obs}(t_k), {}_{t_k}p_x(0), t_k \right) - p_0\left({}_{t_k}p_x^{obs}(t_k), {}_{t_k}p_x(0), t_k \right) \right], \end{aligned} \tag{36}$$

where $c_0(\cdot)$ and $p_0(\cdot)$ are given by equations (14) and (27), respectively.

As shown in Subsection 2.1, the importance of the longevity option decomposition approach for pricing index-based longevity swaps and other longevity-linked securities is that

S-forwards, q-forwards, longevity caplets and longevity floorlets constitute the basic building blocks from which any more complex longevity- or mortality-related derivative security can be structured and priced. Although indexed-based longevity hedges based on a broad-based reference population longevity index carry some basis risk, when appropriately designed to closely match the mortality experience of the liability portfolio, a series of S-forwards (i.e., a portfolio of longevity caplets and floorlets) can be used to hedge the longevity exposure of an annuity book or of a pension liability with greater liquidity and transparency than bespoke insurance-based hedging solutions.

More generally, some investors may be interested in speculating against future longevity developments by entering into a longevity swap. For example, an investor who expects survival rates of a given cohort to increase more (less) than what is currently anticipated should enter into a long (short) longevity swap position, leading to positive cash flows over time if the actual survival rates turn out to be higher (lower) than expected.

2.5. Characteristic function

The implementation of Proposition 1 only requires two ingredients: the knowledge of the characteristic function (18) and the identification of the optimal dampening parameter α.

Concerning the first ingredient, next proposition is inspired on Lamberton and Lapeyre (1996) and Cont and Tankov (2004), and shows that the characteristic function (18) can be always obtained as the solution of a partial integro-differential equation (PIDE).

Proposition 4 *Assume that the mortality intensity of an individual aged $x+t$ at time t, $\mu_{x+t}(t)$, is driven, under the forward probability measure $\mathbb{Q}_T$, by the jump-diffusion process*

$$d\mu_{x+t}(t) = m\left(t, \mu_{x+t}(t)\right) dt + n\left(t, \mu_{x+t}(t)\right) dW_t^{\mathbb{Q}_T} + dJ_t^{\mathbb{Q}_T}, \tag{37}$$

where $m\left(t, \mu_{x+t}(t)\right) \in \mathbb{R}$ and[8] *$n\left(t, \mu_{x+t}(t)\right) \in \mathbb{R}$ satisfy the usual Lipschitz and growth conditions, $\left\{W_t^{\mathbb{Q}_T} : t \geq 0\right\}$ is a $\mathbb{Q}_T$-measured standard Brownian motion, and*

$$J_t^{\mathbb{Q}_T} = \sum_{i=1}^{N_t^{\mathbb{Q}_T}} Y_i^{\mathbb{Q}_T} \tag{38}$$

[8] The analysis could be easily extended for $n\left(t, \mu_{x+t}(t)\right) \in \mathbb{R}^{n \times n}$ with $n > 1$, that is for the case where the mortality intensity is driven by n (> 1) Brownian motions.

is a compound Poisson process such that $\left\{N_t^{\mathbb{Q}_T} : t \geq 0\right\}$ *is a* $\mathbb{Q}_T$*-measured standard Poisson process with intensity* $\bar{\eta} \in \mathbb{R}$*, and the jump sizes* $\left\{Y_i^{\mathbb{P}}\right\}_{i=1}^{\infty}$ *are independent and identically distributed (i.i.d.) random variables with density* f_Y *and mean* $\zeta \in \mathbb{R}$*. All Wiener, Poisson and jump size processes are taken as independent from each other. Then, the characteristic function (18) solves the PIDE*

$$
\begin{aligned}
0 \;=\; & -i\phi\mu_{x+t}(t)\,\tilde{g}\left(t,T;\phi;\mu_{x+t}(t)\right) + \frac{\partial \tilde{g}\left(t,T;\phi;\mu_{x+t}(t)\right)}{\partial t} \\
& + m\left(t,\mu_{x+t}(t)\right)\frac{\partial \tilde{g}\left(t,T;\phi;\mu_{x+t}(t)\right)}{\partial \mu_{x+t}(t)} + \frac{1}{2}n^2\left(t,\mu_{x+t}(t)\right)\frac{\partial^2 \tilde{g}\left(t,T;\phi;\mu_{x+t}(t)\right)}{\partial \mu_{x+t}(t)^2} \\
& + \bar{\eta}\int_{-\infty}^{\infty}\left[\tilde{g}\left(t,T;\phi;\mu_{x+t}(t)+y\right) - \tilde{g}\left(t,T;\phi;\mu_{x+t}(t)\right)\right] f_Y(y)\,dy,
\end{aligned}
\tag{39}
$$

subject to the terminal condition

$$\tilde{g}\left(T,T;\phi;\mu_{x+T}(T)\right) = 1, \tag{40}$$

and where

$$\tilde{g}\left(t,T;\phi;\mu_{x+t}(t)\right) := g\left(t,T;\phi;\mu_{x+t}(t)\right) \times \left({}_{T-t}p_{x+t}(t)\right)^{i\phi}. \tag{41}$$

Proof. Please see Section B of the supplementary file. ■

Furthermore, and following, for instance, Björk (1998) or Duffie et al. (2000), the PIDE (39) can be decomposed into a simpler system of ordinary differential equations (ODEs) if both the drift and the squared diffusion of the stochastic differential equation (37) are specified as affine functions of the mortality intensity $\mu_{x+t}(t)$.[9]

Proposition 5 *Under the assumptions of Proposition 4, and if*

$$m\left(t,\mu_{x+t}(t)\right) = \bar{b} + \bar{a}\mu_{x+t}(t), \tag{42}$$

and

$$n\left(t,\mu_{x+t}(t)\right) = \sqrt{d + c\mu_{x+t}(t)}, \tag{43}$$

for $\bar{a}, \bar{b} \in \mathbb{R}$ *and* $c, d \in \mathbb{R}_+$*, then the characteristic function (18) is equal to*

$$g\left(t,T;\phi;\mu_{x+t}(t)\right) = \frac{\exp\left[\theta(t,T;\phi) + \beta(t,T;\phi)\,\mu_{x+t}(t)\right]}{\left({}_{T-t}p_{x+t}(t)\right)^{i\phi}}, \tag{44}$$

[9]Note that the jump intensity $\bar{\eta}$ is already assumed to be a constant.

where $\theta(t,T;\phi), \beta(t,T;\phi) \in \mathbb{C}$ *solve the complex-valued ODEs*

$$\frac{\partial \beta(t,T;\phi)}{\partial t} = i\phi - \bar{a}\beta(t,T;\phi) - \frac{1}{2}c\beta^2(t,T;\phi), \tag{45}$$

and

$$\frac{\partial \theta(t,T;\phi)}{\partial t} = -\bar{b}\beta(t,T;\phi) - \frac{1}{2}d\beta^2(t,T;\phi) - \bar{\eta}\int_{-\infty}^{\infty}\left[e^{\beta(t,T;\phi)y} - 1\right] f_Y(y)\,dy, \tag{46}$$

subject to the boundary conditions

$$\theta(T,T;\phi) = 0, \tag{47}$$

and

$$\beta(T,T;\phi) = 0. \tag{48}$$

Proof. Please see Section C of the supplementary file. ■

The Riccati differential equation (45) can be numerically solved through, for instance, a *Runge-Kutta method*—as described in Press et al. (1994, Section 15.2)—, and then function $\theta(t,T;\phi)$ follows by numerical integration of the ordinary differential equation (46). Nevertheless, Proposition 6 will soon offer a much more efficient alternative: a closed-form solution for both complex-valued functions $\beta(t,T;\phi)$ and $\theta(t,T;\phi)$.

3. Analytical pricing of longevity derivatives

Given the reduced liquidity of the longevity derivatives market, any mortality model must be calibrated to mortality data. Hence, the mortality model (37), (42) and (43) will be now specified under the real world (or physical) measure $\mathbb{P}$, and a rather general density of jump sizes is also adopted.

3.1. Mortality model

Hereafter, and under the physical probability measure $\mathbb{P}$, the mortality intensity of an individual aged $x+t$ at time t, $\mu_{x+t}(t)$, is driven by the affine jump-diffusion process

$$d\mu_{x+t}(t) = \left[b + a\mu_{x+t}(t)\right]dt + \sqrt{d + c\mu_{x+t}(t)}\,dW_t^{\mathbb{P}} + d\left(\sum_{i=1}^{N_t^{\mathbb{P}}} Y_i^{\mathbb{P}}\right), \tag{49}$$

where $\mu_x(0) > 0$, $a, b \in \mathbb{R}$, $c, d \in \mathbb{R}_+$, $\{W_t^{\mathbb{P}} : t \geq 0\}$ is a $\mathbb{P}$-measured standard Brownian motion, and $\{N_t^{\mathbb{P}} : t \geq 0\}$ is a $\mathbb{P}$-measured standard Poisson process with intensity η. The jump sizes $\{Y_i^{\mathbb{P}}\}_{i=1}^{\infty}$ are i.i.d. random variables with the asymmetric double exponential density of Kou and Wang (2004):

$$f(y) := \frac{\pi_1}{\upsilon_1} e^{-\frac{y}{\upsilon_1}} \mathbb{1}_{\{y \geq 0\}} + \frac{\pi_2}{\upsilon_2} e^{\frac{y}{\upsilon_2}} \mathbb{1}_{\{y < 0\}}, \tag{50}$$

where $\pi_1, \pi_2 \geq 0$, $\frac{1}{\upsilon_1} > 1$, $\upsilon_2 > 0$, and $\pi_1 + \pi_2 = 1$. The variables π_1 and π_2 represent, respectively, the probabilities of a positive (with average size $\frac{1}{\upsilon_1} > 0$) and negative (with average absolute size $\frac{1}{\upsilon_2} > 0$) jump in mortality. By setting $\pi_1 = 0$ we are interested only on the importance of longevity risk—see, e.g., Biffis (2005). When $\upsilon_1 = \upsilon_2$ and $\pi_1 = \pi_2 = \frac{1}{2}$ we get the so-called "first Laplace law". All sources of randomness—$\{W_t^{\mathbb{P}} : t \geq 0\}$, $\{N_t^{\mathbb{P}} : t \geq 0\}$, and $\{Y_i^{\mathbb{P}}\}_{i=1}^{\infty}$—are assumed to be independent.

In opposition to previous approaches that focused almost exclusively on describing longevity risk, our model accounts for both negative and positive mortality jumps, offering a richer and flexible approach for the valuation of any longevity-linked security. The negative jumps in the process (49) represent mortality improvements (e.g., new rare medical breakthroughs), whereas positive jumps represent a deterioration in the survival schedule.

The stochastic process (49) is very general and encompasses, as special cases, several mortality models already proposed in the literature. Nevertheless, and based on economic and demographic arguments, we advocate, as our "baseline model", a non-mean reverting square-root affine jump-diffusion process combined with a Poisson process with double asymmetric exponentially distributed jumps, i.e., the process (49) subject to two restrictions: $b = d = 0$. Under our "baseline model", the deterministic part of the process (49) increases exponentially with age, as observed at adult ages in most countries, and follows the Gompertz law in expected terms. Moreover, the use of a non-mean reverting stochastic process is validated by empirical studies—see, e.g., Luciano and Vigna (2008) or Bravo (2007, 2011)—and departs, for instance, from Zeddouk and Devolder (2019), who consider two mean-reverting affine stochastic processes with no jump component. Two additional advantages of our "baseline model" are: first, the mortality intensity cannot become negative with positive probability, provided that the starting point is nonnegative; and, second, that in calibration exercises (considering adult ages) the survival probability is decreasing at every age, a desirable biologically reasonable feature.[10]

To price longevity derivatives, the stochastic differential equation (49) must be rewritten under the pricing measure $\mathbb{Q}$, i.e., under the equivalent martingale measure associated to the numeraire "money-market account". Such measure exists—since no-arbitrage is being assumed—but is not unique—because the longevity market under analysis is incomplete and, hence, there are no restrictions on the specification adopted for the market price of longevity risk. Concerning the diffusive component of the longevity risk, and for analytical convenience, we will assume that

$$dW_t^{\mathbb{Q}} = dW_t^{\mathbb{P}} + \lambda_d \sqrt{d + c\mu_{x+t}(t)} \tag{51}$$

is a standard Brownian motion increment under the martingale measure $\mathbb{Q}$, for $\lambda_d \in \mathbb{R}$.

The jump component of the longevity risk is accounted for through a new $\mathbb{Q}$-measured standard Poisson process $\left\{N_t^{\mathbb{Q}} : t \geq 0\right\}$ with intensity $\bar{\eta}$, and new i.i.d. jump sizes $\left\{Y_i^{\mathbb{Q}}\right\}_{i=1}^{\infty}$ with a different asymmetric double exponential density

$$f(y) := \frac{\bar{\pi}_1}{\bar{v}_1} e^{-\frac{y}{\bar{v}_1}} \mathbb{1}_{\{y \geq 0\}} + \frac{\bar{\pi}_2}{\bar{v}_2} e^{\frac{y}{\bar{v}_2}} \mathbb{1}_{\{y < 0\}}, \tag{52}$$

where $\bar{\pi}_1, \bar{\pi}_2 \geq 0$, $\frac{1}{\bar{v}_1} > 1$, $\bar{v}_2 > 0$, and $\bar{\pi}_1 + \bar{\pi}_2 = 1$. Again, all sources of randomness—$\left\{W_t^{\mathbb{Q}} : t \geq 0\right\}$, $\left\{N_t^{\mathbb{Q}} : t \geq 0\right\}$, and $\left\{Y_i^{\mathbb{Q}}\right\}_{i=1}^{\infty}$—are assumed to be independent. In summary, and under the pricing measure $\mathbb{Q}$, the mortality intensity of an individual aged $x + t$ at time t is driven by the following affine jump-diffusion process (with finite activity):

$$d\mu_{x+t}(t) = \left[\bar{b} + \bar{a}\mu_{x+t}(t)\right] \mu_{x+t}(t)\, dt + \sqrt{d + c\mu_{x+t}(t)}\, dW_t^{\mathbb{Q}} + d\left(\sum_{i=1}^{N_t^{\mathbb{Q}}} Y_i^{\mathbb{Q}}\right), \tag{53}$$

with

$$\bar{a} := a - c\lambda_d, \tag{54}$$

and

$$\bar{b} := b - d\lambda_d. \tag{55}$$

[10] Although, in theoretical terms, the negative jumps in the stochastic process increase the likelihood of the intensity to become negative, in empirical calibration exercises the probability of negative values can be considered negligible.

3.2. Financial markets

Since longevity derivatives can have long maturities, it is important to ensure a good model fit to the current term structure of interest rates. Therefore, an Heath et al. (1992) model—that guarantees an automatic fit to the observed yield curve—will be adopted hereafter. Formally, we assume that

$$\frac{dP(t,T)}{P(t,T)} = r_t dt + \sigma(t,T)' \cdot dZ_t^{\mathbb{Q}}, \tag{56}$$

where $\cdot$ denotes the inner product in $\mathbb{R}^n$, and $\left\{Z_t^{\mathbb{Q}} \in \mathbb{R}^n : t \geq 0\right\}$ is a n-dimensional standard Brownian motion, initialized at zero and generating the augmented, right continuous and complete filtration $\mathbb{F} = \{\mathcal{F}_t : t \geq 0\}$. The n-dimensional adapted volatility function $\sigma(\cdot, T) : [0,T] \to \mathbb{R}^n$ is assumed to satisfy the usual mild measurability and integrability requirements—as stated, for instance, in Lamberton and Lapeyre (1996)—as well as the boundary condition $\sigma(u,u) = \underline{0} \in \mathbb{R}^n, \forall u \in [0,T]$, and can be either deterministic or stochastic since following, for instance, Schräger (2006), we assume independence between financial markets and mortality:

Assumption 1 *All sources of randomness—* $\left\{W_t^{\mathbb{Q}} : t \geq 0\right\}$*,* $\left\{N_t^{\mathbb{Q}} : t \geq 0\right\}$*,* $\left\{Y_i^{\mathbb{Q}}\right\}_{i=1}^{\infty}$ *and* $\left\{Z_t^{\mathbb{Q}} \in \mathbb{R}^n : t \geq 0\right\}$ *— are independent.*

Given that the characteristic function (18) is defined under the forward measure $\mathbb{Q}_T$, our pricing model must be specified under the same equivalent martingale measure. For this purpose, and following, for instance, Nunes (2004, Equation 2.8), it is well known that the *Radon-Nikodym derivative* of $\mathbb{Q}_T$ with respect to $\mathbb{Q}$ is equal to

$$\left.\frac{d\mathbb{Q}_T}{d\mathbb{Q}}\right| \mathcal{F}_t = \exp\left[\int_0^t \sigma(s,T)' \cdot dZ_s^{\mathbb{Q}} - \frac{1}{2}\int_0^t \|\sigma(s,T)\|^2 ds\right], \tag{57}$$

where $\|\cdot\|$ denotes the Euclidean norm in $\mathbb{R}^n$. Therefore, Girsanov's theorem implies that

$$dZ_t^{\mathbb{Q}_T} = dZ_t^{\mathbb{Q}} - \sigma(t,T)\,dt, \tag{58}$$

is a standard Brownian motion increment (in $\mathbb{R}^n$) under the equivalent forward measure $\mathbb{Q}_T$, while the stochastic differential equation followed by the mortality intensity under measure $\mathbb{Q}_T$ is exactly the same as the one followed under measure $\mathbb{Q}$—i.e. equation (53)—because $W_t^{\mathbb{Q}} = W_t^{\mathbb{Q}_T}$, $N_t^{\mathbb{Q}} = N_t^{\mathbb{Q}_T}$, and $Y_i^{\mathbb{Q}} = Y_i^{\mathbb{Q}_T}$, for all t and i.

Longevity derivatives allow pension schemes and annuity providers to hedge longevity risk but introduce bilateral counterparty credit risk to the extent that the risk is not mitigated or eliminated by collateralization. In this paper we do not consider the impact of counterparty risk and collateralization on longevity derivatives valuation.[11]

3.3. Analytical expression of the characteristic function

Even though we prescribe a restricted specification with $\bar{b} = d = 0$, next proposition shows that it is possible to obtain an explicit solution for the ODEs (45) and (46) under the most general affine jump-diffusion mortality (pricing) model proposed in this paper.

Proposition 6 *Under the pricing model defined by equations (52), (53), (56) and (58) as well as by Assumption 1, the characteristic function (18) is given by equation (44), where*

$$\beta(t,T;\phi) = \frac{[\bar{a} - h(\phi)]\{\exp[h(\phi)(T-t)] - 1\}}{c\{1 - q(\phi)\exp[h(\phi)(T-t)]\}}, \tag{59}$$

and

$$\theta(t,T;\phi) = \theta_{\beta}(t,T;\phi) + \theta_{\beta^2}(t,T;\phi) + \theta_J(t,T;\phi), \tag{60}$$

with

$$\theta_{\beta}(t,T;\phi) = \frac{\bar{b}[\bar{a} - h(\phi)]}{c}\left[\frac{q(\phi) - 1}{h(\phi)q(\phi)}\ln\left(\frac{q(\phi)\exp[h(\phi)(T-t)] - 1}{q(\phi) - 1}\right) - (T-t)\right], \tag{61}$$

$$\begin{aligned} &\theta_{\beta^2}(t,T;\phi) \\ = \;& \frac{d[\bar{a} - h(\phi)]^2}{2c^2}\Bigg\{(T-t) \\ &+\frac{\left[1 - q^2(\phi) + \left(q^3(\phi) - q(\phi)\right)e^{h(\phi)(T-t)}\right]\ln\left(\frac{q(\phi)e^{h(\phi)(T-t)} - 1}{q(\phi)}\right) + 1 - 2q(\phi) + q^2(\phi)}{h(\phi)q^2(\phi)\left[1 - q(\phi)e^{h(\phi)(T-t)}\right]} \\ &-\frac{\left[1 - q^2(\phi) + q^3(\phi) - q(\phi)\right]\ln\left(\frac{q(\phi) - 1}{q(\phi)}\right) + 1 - 2q(\phi) + q^2(\phi)}{h(\phi)q^2(\phi)[1 - q(\phi)]}\Bigg\}, \end{aligned} \tag{62}$$

[11]For a detailed analysis on the impact of bilateral default risk and collateral rules on the marking to market of longevity swaps see, for instance, Biffis et al. (2016).

$$
\begin{aligned}
&\theta_J(t,T;\phi) \quad (63)\\
=\;& \left\{ \frac{\bar{\eta}\bar{\pi}_1 c}{c+\bar{v}_1\left[\bar{a}-h(\phi)\right]} + \frac{\bar{\eta}\bar{\pi}_2 c}{c-\bar{v}_2\left[\bar{a}-h(\phi)\right]} - \bar{\eta} \right\}(T-t)\\
&-\bar{\eta}\bar{\pi}_1 c \frac{\frac{cq(\phi)+\bar{v}_1[\bar{a}-h(\phi)]}{c+\bar{v}_1[\bar{a}-h(\phi)]} - q(\phi)}{h(\phi)\left\{cq(\phi)+\bar{v}_1\left[\bar{a}-h(\phi)\right]\right\}}\\
&\times \ln \frac{\left[c+\bar{v}_1\left(\bar{a}-h(\phi)\right)\right] - \left[cq(\phi)+\bar{v}_1\left(\bar{a}-h(\phi)\right)\right]e^{h(\phi)(T-t)}}{c\left[1-q(\phi)\right]}\\
&-\bar{\eta}\bar{\pi}_2 c \frac{\frac{cq(\phi)-\bar{v}_2[\bar{a}-h(\phi)]}{c-\bar{v}_2[\bar{a}-h(\phi)]} - q(\phi)}{h(\phi)\left\{cq(\phi)-\bar{v}_2\left[\bar{a}-h(\phi)\right]\right\}}\\
&\times \ln \frac{\left[c-\bar{v}_2\left(\bar{a}-h(\phi)\right)\right] - \left[cq(\phi)-\bar{v}_2\left(\bar{a}-h(\phi)\right)\right]e^{h(\phi)(T-t)}}{c\left[1-q(\phi)\right]},
\end{aligned}
$$

$$
h(\phi) := \sqrt{\bar{a}^2 + 2ci\phi}, \quad (64)
$$

and

$$
q(\phi) := \frac{\bar{a}-h(\phi)}{\bar{a}+h(\phi)}. \quad (65)
$$

Proof. Please see Section D of the supplementary file. ∎

3.4. Optimal integration contour

For models like the one specified in equation (53) that have an analytically available characteristic function, Fourier inversion offers a fast and efficient computational method for pricing plain vanilla options. In order to improve the numerical stability of the Fourier inversion, Lord and Kahl (2007) suggest a method to find the optimal contour of integration. More specifically, the dampening parameter $\alpha \in \mathbb{R}$ must ensure that the integrand

$$
\psi(u,\alpha) := e^{-\alpha\varpi}\,\mathrm{Re}\left[e^{-iu\varpi}\varsigma(0,T;u;\alpha)\right] \quad (66)
$$

in equation (22) is finite; that is, and since the maximum value of the integrand function (66) occurs at $u=0$, it is enough to ensure that $\psi(0,\alpha)<\infty$, i.e. that

$$
\mathbb{E}_{\mathbb{Q}_T}\left[I_x(0,T)^{\alpha+1} \middle| \mathcal{H}_0 \right] < \infty. \quad (67)
$$

Therefore, and following Lord and Kahl (2007), the optimal $\alpha^* \in \mathbb{R}$ that ensures the stability of the integrand function (66) over the whole integration domain is found as

$$
\alpha^* = \arg \min_{\alpha\in[\alpha_{\min},\alpha_{\max}]} \left| -\alpha\varpi + \frac{1}{2}\ln \mathrm{Re}\left[\varsigma(0,T;0;\alpha)\right]^2 \right|, \quad (68)
$$

where the interval $[\alpha_{\min}, \alpha_{\max}]$ corresponds to the strip of regularity for the characteristic function (18).

To define $\alpha_{\min}$ and $\alpha_{\max}$, note that the compound Poisson process (38) and the Brownian motion $\left\{W_t^{\mathbb{Q}_T} : t \geq 0\right\}$ are assumed to be independent, and, therefore, the characteristic function offered by equations (44), (59) and (60) can be factorized into

$$g\left(t, T; \phi; \mu_{x+t}(t)\right) = \frac{g_D(\phi) \times g_J(\phi)}{\left({}_{T-t}p_{x+t}(t)\right)^{i\phi}}, \tag{69}$$

where

$$g_D(\phi) := \exp\left[\beta(t, T; \phi)\, \mu_{x+t}(t) + \theta_\beta(t, T; \phi) + \theta_{\beta^2}(t, T; \phi)\right] \tag{70}$$

is the factor associated to the diffusion component of the model, and

$$g_J(\phi) := \exp\left[\theta_J(t, T; \phi)\right] \tag{71}$$

is the factor related to the jump component of the pricing model. For each component (70) or (71), the goal is to define the range of $\alpha \in \mathbb{R}$ values that satisfies condition (67).

Using equations (18) and (44), condition (67) can be restated as

$$\begin{aligned}
\mathbb{E}_{\mathbb{Q}_T}\left[e^{(\alpha+1)z_x(t,T)} \middle| \mathcal{H}_t\right] &= g\left(t, T; -i(\alpha+1); \mu_{x+t}(t)\right) \\
&= \frac{\exp\left[\theta(t, T; -i(\alpha+1)) + \beta(t, T; -i(\alpha+1))\, \mu_{x+t}(t)\right]}{\left({}_{T-t}p_{x+t}(t)\right)^{i\phi}} \\
&< \infty.
\end{aligned} \tag{72}$$

Starting with the diffusion component, and defining

$$\tau := T - t, \tag{73}$$

equation (45) implies that $\beta(t, T; -i(\alpha+1))$ must be such that

$$\begin{aligned}
\frac{\partial \beta(t, T; -i(\alpha+1))}{\partial \tau} &= -(\alpha+1) + \bar{a}\beta(t, T; -i(\alpha+1)) + \frac{c}{2}\beta^2(t, T; -i(\alpha+1)) \\
&= \frac{c}{2} h\left(\beta(t, T; -i(\alpha+1))\right)
\end{aligned} \tag{74}$$

and $\beta(t, T; -i(\alpha+1)) = 0$, where the quadratic function $h(y) := y^2 + \tilde{a}y + \tilde{b}$ is defined as in Andersen and Piterbarg (2007), while

$$\tilde{a} := \frac{2\bar{a}}{c}, \tag{75}$$

and

$$\tilde{b} := -\frac{2(\alpha+1)}{c}. \tag{76}$$

The stability of the integrand function (66) depends on the non-explosion of the Riccati differential equation (74), and the range of values of τ (as a function of $\alpha+1$) for which this is accomplished is offered by Andersen and Piterbarg (2007, Proposition 3.1) that is now summarized (for the sake of completeness):

Proposition 7 *For*

$$D(\alpha+1) := \tilde{a}^2 - 4\tilde{b}, \tag{77}$$

condition (72) is met for all $\tau < \tau^*(\alpha+1)$*, where:*

1. *For* $D(\alpha+1) \geq 0$ *and* $\tilde{a} < 0$, $\tau^*(\alpha+1) = \infty$*;*
2. *For* $D(\alpha+1) \geq 0$ *and* $\tilde{a} > 0$,
$$\tau^*(\alpha+1) = \frac{2}{c\sqrt{D(\alpha+1)}} \ln\left(\frac{\tilde{a}+\sqrt{D(\alpha+1)}}{\tilde{a}-\sqrt{D(\alpha+1)}}\right); \tag{78}$$
3. *For* $D < 0$,
$$\tau^*(\alpha+1) = \frac{4}{c\sqrt{-D(\alpha+1)}}\left(\pi \mathbb{1}_{\{\tilde{a}<0\}} + \arctan\left(\frac{\sqrt{-D(\alpha+1)}}{\tilde{a}}\right)\right). \tag{79}$$

Proof. This result is borrowed from Andersen and Piterbarg (2007, Proposition 3.1). ■

Therefore, the optimal $\alpha \in \mathbb{R}$ will be found through the minimization problem (68) but subject to the stability condition

$$\tau^*(\alpha+1) \geq \tau, \tag{80}$$

and initialized at the level α such that $\tau^*(\alpha+1) = \tau$.

Concerning the factor (71) related to the jump component of the pricing model, and as noted by Lord and Kahl (2007, Section 3.1.2), such factor is always finite; the only problem being that it might exceed the largest finite number L representable on the computer system.[12] Hence, an additional constraint is added to the minimization problem (68) and (80):

$$|\theta(t, T; -i(\alpha+1))| \leq \frac{1}{4}\ln(L). \tag{81}$$

[12] For instance, L is the largest finite floating-point number in IEEE double precision, denoted by "realmax" in *Matlab*.

4. Empirical results

This section describes the model calibration approach and provides illustrative results on the valuation of longevity swaps, caplets and floorlets using U.S. mortality data.

4.1. Model calibration

To estimate the parameters that determine the dynamics of the mortality intensity process (49), we follow a cohort approach and use the U.S. total population mortality data from 1950 to 2017, and for ages in the range 65-100. Mortality data is obtained from the Human Mortality Database (2019). For the discretized stochastic process, we assume that the age-specific forces of mortality are constant within yearly bands of time and age, i.e., within each square of the Lexis diagram. Formally, given any integer age x and calendar year t, we assume that $\mu_{x+\xi}(t+\tau)=\mu_x(t)$ for any $0\leq\xi,\tau<1$. Under this assumption, the mortality intensity is approximated by the central death rate $m_x(t)$ and the one-year survival probability is given by $p_x(t)=\exp(-m_x(t))$. From the central death rates, we obtain empirical survival curves for representative cohorts using

$$ {}_{T-t}p_{x+t}^{obs}(t)\approx\exp\left(-\sum_{j=0}^{T-1}m_{x+j}(t+j)\right). \tag{82}$$

To calibrate the mortality process (49) to data, it is convenient to consider the model survival probabilities instead of the mortality intensity. For this purpose, the $(T-t)$-year survival probability of an individual aged $x+t$ at time t can be stated as

$$ {}_{T-t}p_{x+t}(t):=\mathbb{E}_{\mathbb{P}}\left[\exp\left(-\int_t^T\mu_{x+s}(s)\,ds\right)\middle|\mathcal{G}_t\right]. \tag{83}$$

The convenience of adopting the affine jump-diffusion process (49) in modelling the mortality intensity comes from the fact that, under certain technical conditions—described, for instance, in Duffie et al. (2000)—, the survival probability (83) is given by the closed-form solution offered by Bravo (2007, 2011). More specifically, and comparing equations (18), (41) and (83), it follows that the survival probability can be obtained from the analytical solution offered in Proposition 6 for the characteristic function, after equating to zero all market prices of risk, i.e.

$$ {}_{T-t}p_{x+t}(t)=\tilde{g}\left(t,T;-i;\mu_{x+t}(t)\right)\big|_{\lambda_d=0}. \tag{84}$$

Table 1: Parameters for different cohorts and for different model specifications.

Model	Parameters								Fit measures		
	a	b	$\sqrt{c}$	η	v_1	v_2	π_1	$\mu_{65}(0)$	MSE	AIC	BIC
	Panel A: Cohort aged 65 in 1950										
Feller with jumps	0.075408		0.009748	0.099831	0.001000	0.000824	0.000100	0.028838	0.0000608	-139.78	-142.44
OU	0.072372		0.000100					0.028838	0.0000685	-145.91	-146.79
OU with jumps	0.072391		0.000100	0.009997	0.001000	0.001000	0.000100	0.028838	0.0000664	-138.40	-141.06
Vasicek	-0.001864	0.003758	0.000010					0.028838	0.0010519	-101.21	-102.54
CIR	-0.000455	0.003691	0.000010					0.028838	0.0010240	-101.63	-102.96
	Panel B: Cohort aged 65 in 1960										
Feller with jumps	0.072387		0.000906	0.100000	0.001000	0.003514	0.000100	0.028696	0.0000910	-133.47	-136.14
OU	0.064726		0.000100					0.028696	0.0000955	-140.72	-141.60
OU with jumps	0.064745		0.000100	0.009994	0.001000	0.001000	0.000100	0.028696	0.0000933	-133.08	-135.74
Vasicek	-0.001578	0.003181	0.000010					0.028696	0.0010563	-101.14	-102.48
CIR	-0.000454	0.003685	0.000010					0.028696	0.0010338	-101.48	-102.81
	Panel C: Cohort aged 65 in 1970										
Feller with jumps	0.078929		0.000100	0.250000	0.000994	0.002574	0.000100	0.026139	0.0002343	-118.69	-121.35
OU	0.063934		0.000100					0.026139	0.0003426	-120.75	-121.63
OU with jumps	0.076630		0.000100	0.254200	0.000764	0.000782	0.001936	0.026139	0.0002368	-118.52	-121.18
Vasicek	-0.001591	0.002929	0.000100					0.026139	0.0018130	-92.70	-94.03
CIR	-0.000403	0.002874							0.0017804	-92.98	-94.31

continues on the next page

Table 1: (continued)

Model	Parameters								Fit measures		
	a	b	$\sqrt{c}$	η	v_1	v_2	π_1	$\mu_{65}(0)$	MSE	AIC	BIC
	Panel D: Cohort aged 65 in 1980										
Feller with jumps	0.090012		0.000947	0.260000	0.001000	0.002203	0.000100	0.021235	0.0002036	-120.88	-123.55
OU	0.073882		0.000100					0.021235	0.0002269	-127.19	-128.08
OU with jumps	0.073905		0.000100	0.009927	0.001000	0.001000	0.000100	0.021235	0.0002165	-119.92	-122.59
Vasicek	-0.001736	0.003058	0.000039					0.021235	0.0021165	-90.28	-91.61
CIR	-0.000418	0.003003	0.000010					0.021235	0.0020732	-90.60	-91.93
	Panel E: Cohort aged 65 in 1990										
Feller with jumps	0.089403		0.000918	0.280000	0.001000	0.001829	0.000100	0.018787	0.0000315	-150.08	-152.75
OU	0.071353		0.000100					0.018787	0.0000892	-141.79	-142.67
OU with jumps	0.087706		0.000100	0.214200	0.000755	0.000762	0.002145	0.018787	0.0000392	-146.64	-149.30
Vasicek	-0.001820	0.002419	0.000306					0.018787	0.0009829	-102.27	-103.60
CIR	-0.000437	0.002370	0.000010					0.018787			

This table reports the model parameters estimated via equation (85) for the process (49)-(50), using U.S. total population mortality data from the Human Mortality Database (2019), and under different model specifications: our baseline model ("Feller with jumps"), a OU process without mean-reversion or jumps, a OU process without mean-reversion but with double exponential jumps, a Vasiček (1977) process and a Cox et al. (1985) process. For each model specification, three goodness of fit measures are provided in the last three columns: the mean square error (MSE), the Akaike information criterion (AIC), and the Bayesian information criterion (BIC).

Figure 1: Survival probabilities.

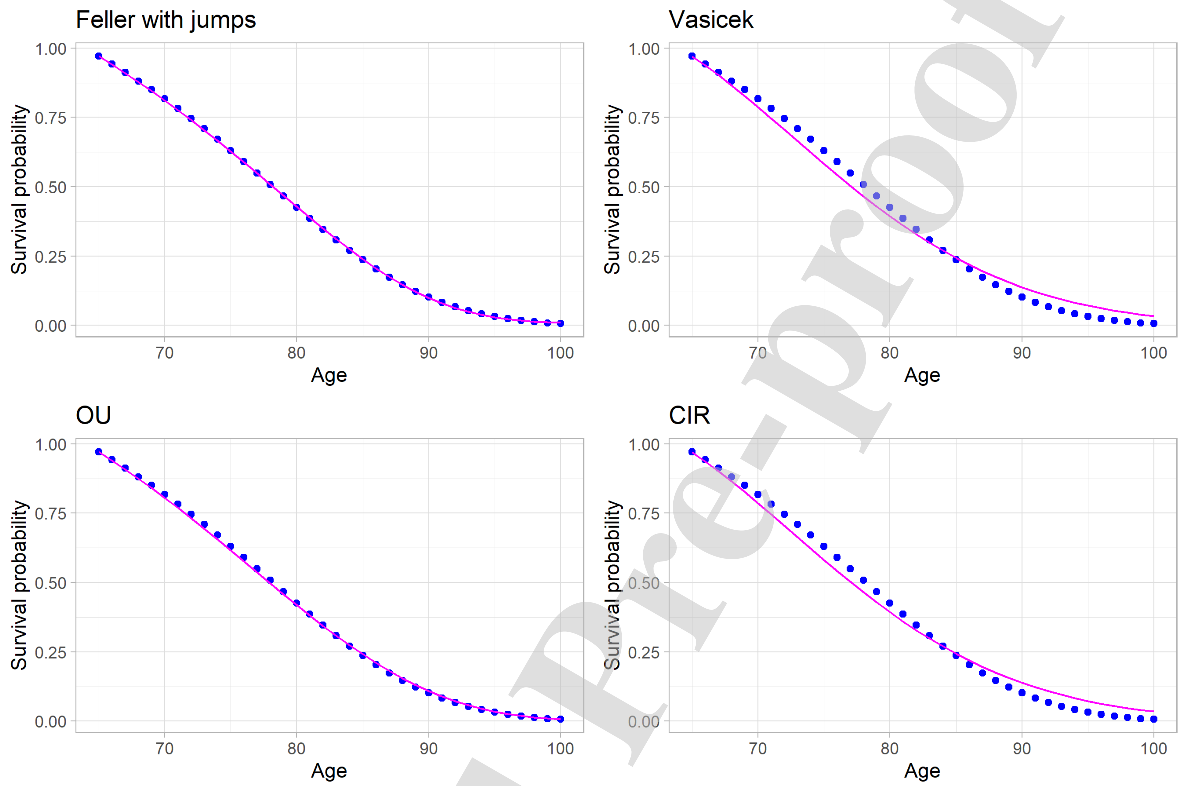

This figure shows the empirical (blue dots) and fitted (magenta line) survival probabilities for a U.S. individual aged 65 in 1950, using U.S. mortality data from Human Mortality Database (2019) and four model specifications estimated in Table 1: our baseline model ("Feller with jumps"), a OU process without mean-reversion or jumps, a Vasiček (1977) process and a Cox et al. (1985) process.

For a given reference cohort x and calendar year $t = 0$, the parameters $\{a, b, c, d, \eta, \pi_1, \pi_2, v_1, v_2\}$ are then estimated by fitting the model survival curves to the empirical survival curves using least squares estimation, i.e., by solving

$$\{a, b, c, d, \eta, \pi_1, \pi_2, v_1, v_2\} = \underset{a,b,c,d,\eta,\pi_1,\pi_2,v_1,v_2}{\arg\min} \left(\sum_{T=1}^{\omega - x} \left({}_{T-t}p_{x+t}^{obs}(t) - {}_{T-t}\,p_{x+t}(t) \right)^2 \right). \tag{85}$$

Besides our "baseline model"—a Feller process with jumps, as given by equations (49) and (50) but with $b = d = 0$—, four other nested specifications are also calibrated to the same mortality data: a Ornstein Uhlenbeck (OU) process without mean reversion, with a positive trend and constant volatility ($b = c = \eta = \pi_1 = \pi_2 = v_1 = v_2 = 0$); the same OU process but with double exponential jumps ($b = c = 0$); and the classical Vasiček (1977)—with $c = \eta = \pi_1 = \pi_2 = v_1 = v_2 = 0$—and Cox et al. (1985)—with $d = \eta = \pi_1 = \pi_2 = v_1 = v_2 = 0$—models that assume time-homogeneous mean reverting affine processes without jumps for the mortality intensity. The parameter estimates for all these five affine specifications, as well as the initial value of $\mu_{x+t}(t)$—$\mu_{65}(0)$, that is chosen to be equal to $-\ln(p_{65}(0))$—, are reported in Table 1 for cohorts aged 65 in 1950, 1960, 1970, 1980 and 1990. Additionally, Figure 1 plots the observed (blue dots) and fitted (magenta line) survival probabilities of a U.S. individual aged 65 in 1950 for four of these affine models.

Similarly to previous studies, our results show that the time-homogeneous mean reverting affine processes—the Vasiček (1977) and Cox et al. (1985) models—fail to fit observed survival probabilities and to capture the rectangularization and expansion phenomenon, and should be discarded in pricing and forecasting exercises. The mean square error of the Vasiček (1977) and Cox et al. (1985) models is substantially higher than that of non-mean reverting processes because the force of mortality shows no mean reversion at adult ages, but rather an exponential increase. In all non-mean reverting processes, the mean square errors (MSE) are small, indicating a good fit to observed survival curves. The Feller with jumps process (our "baseline model") exhibits the smallest fitting errors in the five cohorts considered in this study, followed closely by the OU and OU with jumps models. Models with jumps generally fit better than models without jumps. We note, however, that when we compare the maximum likelihoods attained by each model, it is natural for models with more parameters (Feller and OU with jumps) to fit the data more closely. To balance between quality of fit—which can be enhanced by adding in more parameters—and parsimony, we report the BIC and AIC criterion for all models and periods. The results show that when we account for possible overparameterization, the OU model overperforms the Feller model and the OU with jumps in some cohorts. Note, however, that the main drawback of this OU process is that the intensity can become negative with positive probability, although in empirical studies this probability has been found to be negligible—Luciano and Vigna (2008). Nevertheless, an exhaustive and systematic comparison of the fitting and forecasting performance of affine jump diffusion models considering different populations and cohorts is beyond the scope of this paper and will be carried out in a parallel paper.

We further note that in the baseline Feller model the decline in the observed mortality intensity at age 65—$\mu_{65}(0)$—in younger cohorts is accompanied by an increase in the drift coefficient a, which represents the relative rate of increase of the force of mortality of the underlying exponential (Gompertz) model and provides a measure of the mortality trend as captured by the model. The parameter estimates also show that the value of the diffusion coefficient c is very low, particularly when compared with that of both positive and negative average size jumps. The average (absolute) size of negative mortality jumps has been declining for younger generations, potentially signalling a slowdown in longevity improvements, but in compensation the jump intensity estimates are higher for younger cohorts.

4.2. Longevity derivatives prices

Table 2 reports the longevity swap price decomposition of Remark 1, for different tenors (in years) and values of the market price of longevity risk premium, for the U.S. total population aged 65 in 1950, and using the parameters specified in Table 1 for our "baseline model".[13] Without loss of generality, we assume the strike price K equals the fitted survival schedule and consider a flat yield curve at 2% for discounting cash flows. Since the market for longevity derivatives is not liquid enough to infer the values of the risk-adjusted model parameters, and in line with previous studies on the magnitude of the market price of longevity risk premium—see, e.g., Zeddouk and Devolder (2019)—we assume three layers for $k = \lambda_d \sqrt{c} \in \{0.25, 0.5, 0.75\}$. All prices are expressed as a percentage of the notional amount (values in basis points). For every tenor and risk premium level, we determine the optimal dampening parameter α and compute the S-forward price as the fair value of a portfolio comprising a long position in a longevity caplet and a short position in the corresponding longevity floorlet. Since the index-based longevity swap is constructed as a basket of S-forwards, the price of the swap is obtained by summing up the individual S-forward prices. Note that the optimal α values obtained are fairly constant for tenors up to 13 years (for each layer of longevity risk premium) but are crucial to achieve accurate results for longer tenors.

[13]The full set of results for all cohorts studied can be obtained from the authors upon request.

Table 2: Decomposition of longevity swap prices for the U.S. cohort aged 65 in 1950.

Tenor		Optimal α			Longevity caplet			Longevity floorlet			S-forward		
(yrs)	k:	0.25	0.5	0.75	0.25	0.5	0.75	0.25	0.5	0.75	0.25	0.5	0.75
1		-29.019	-27.179	-25.401	52.4	55.5	58.5	52.1	54.8	57.4	0.4	0.7	1.1
2		-29.019	-27.179	-25.401	50.9	54.6	58.1	49.5	51.8	54.0	1.4	2.8	4.2
3		-29.019	-27.179	-25.401	50.6	55.3	59.9	47.5	49.1	50.6	3.1	6.2	9.4
4		-29.019	-27.179	-25.401	51.9	58.1	64.1	46.4	47.0	47.7	5.5	11.0	16.5
5		-29.019	-27.179	-25.401	55.1	63.1	71.0	46.5	46.1	45.6	8.5	17.0	25.4
								5-year longevity swap			19.0	37.8	56.5
6		-29.019	-27.179	-25.401	60.6	70.7	80.8	48.5	46.5	44.6	12.1	24.2	36.1
7		-29.019	-27.179	-25.401	68.8	81.0	93.4	52.6	48.6	45.1	16.3	32.4	48.4
8		-29.019	-27.179	-25.401	80.0	94.1	108.9	59.2	52.7	46.9	20.8	41.5	61.9
9		-29.019	-27.179	-25.401	93.9	109.8	126.7	68.1	58.5	50.2	25.8	51.3	76.5
10		-29.019	-27.179	-25.401	109.6	127.1	146.4	78.6	65.4	54.4	31.0	61.7	92.0
								10-year longevity swap			125.0	248.8	371.4

continues on the next page

Table 2: (continued)

Tenor		Optimal α			Longevity caplet			Longevity floorlet			S-forward		
(yrs)	k:	0.25	0.5	0.75	0.25	0.5	0.75	0.25	0.5	0.75	0.25	0.5	0.75
11		-29.019	-27.179	-25.401	125.1	144.8	166.6	88.6	72.4	58.7	36.4	72.4	107.9
12		-29.019	-27.179	-25.401	138.2	161.2	186.4	96.4	78.0	62.3	41.8	83.2	124.0
13		-29.019	-27.179	-25.401	149.1	175.8	204.7	101.9	81.9	64.8	47.2	93.8	140.0
14		-27.273	-27.179	-45.804	158.8	188.7	222.0	106.4	84.6	66.7	52.3	104.1	155.3
15		-22.258	-23.062	-23.890	167.0	200.0	236.3	109.8	86.3	66.5	57.1	113.7	169.7
								15-year longevity swap			359.9	716.1	1,068.5
16		-18.335	-19.046	-19.779	173.4	209.4	249.0	112.0	87.0	66.2	61.5	122.4	182.8
17		-15.233	-15.862	-16.514	177.9	216.6	259.3	112.8	86.6	65.1	65.2	130.0	194.3
18		-12.754	-13.313	-13.893	180.4	221.4	266.9	112.2	85.3	63.3	68.2	136.1	203.7
19		-10.757	-11.254	-11.771	180.8	223.7	271.6	110.4	83.0	60.8	70.4	140.7	210.8
20		-9.135	-9.578	-10.040	179.0	223.4	273.2	107.3	79.9	57.7	71.7	143.5	215.5
								20-year longevity swap			696.9	1,388.8	2,075.5

This table decomposes longevity swap prices for different tenors (in years) and values of the market price of longevity risk, which is defined as $\lambda_d = \frac{k}{\sqrt{c}}$. Columns 2 to 4 display the optimal dampening parameters obtained as described in Subsection 3.4 and used to price longevity caplets and floorlets. The analysis is run for the U.S. total population cohort aged 65 in 1950, using the "baseline model" parameters specified in Table 1, a flat yield curve (with continuous compounding) at 2% per year, and assuming strike prices K equal to the fitted survival schedule shown in Figure 1. All prices are expressed in basis points and as a percentage of the swap notional amount.

Table 2 shows, as expected, that the prices of longevity swaps, S-forwards and longevity options (caplets and floorlets) are increasing in the maturity of the contract and in the market price of longevity risk premium. For instance, the fair value of a 5-year index-based longevity swap with $k = 0.25$ is 19 basis points (0.19%) of the notional amount, whereas for a longer maturity (20-year) contract the price increases to almost 7% (696.9 basis points) of the notional. If the longevity risk insurer demands a higher compensation for taking the uncertainty regarding the future survival prospects of the reference population cohort, e.g., for $k = 0.75$, the 5-year and 20-year survivor swap prices increase to 0.565% and 20.755% of the notional amount, respectively.

To gather further insight on the mortality model proposed, Figure 2 exhibits the sensitivity, for each cohort, of longevity swap prices (in basis points) of different maturities to changes in the baseline model parameters. The top left plot shows, as expected, that the longevity swap price increases with the market price of the diffusive longevity risk λ_d, with a more pronounced effect for older cohorts. The top right plot shows that the higher the risk-neutral probability of a negative jump in the mortality intensity (coefficient $\bar{\pi}_2$) the higher the survival probabilities and the higher the longevity swap price. This effect is more significant for younger cohorts than for older cohorts. The bottom left plot shows, as expected, that the higher the coefficient $\bar{v}_2$ the smaller the longevity swap prices, particularly for older generations. This is because the higher the value of $\bar{v}_2$ the smaller $\frac{1}{\bar{v}_2}$ will be, i.e. the smaller the expected average size of negative jumps in the mortality intensity and, thus, the smaller the longevity improvements. Finally, the bottom right plot shows the impact, for each cohort, on the price of the longevity swap due to changes in the diffusive volatility of the mortality intensity. We can observe that due to the smaller magnitude of the c coefficient estimates, the swap price is relatively insensitive to changes in the mortality intensity diffusive volatility.

Figure 2: Simulation analysis of the baseline model

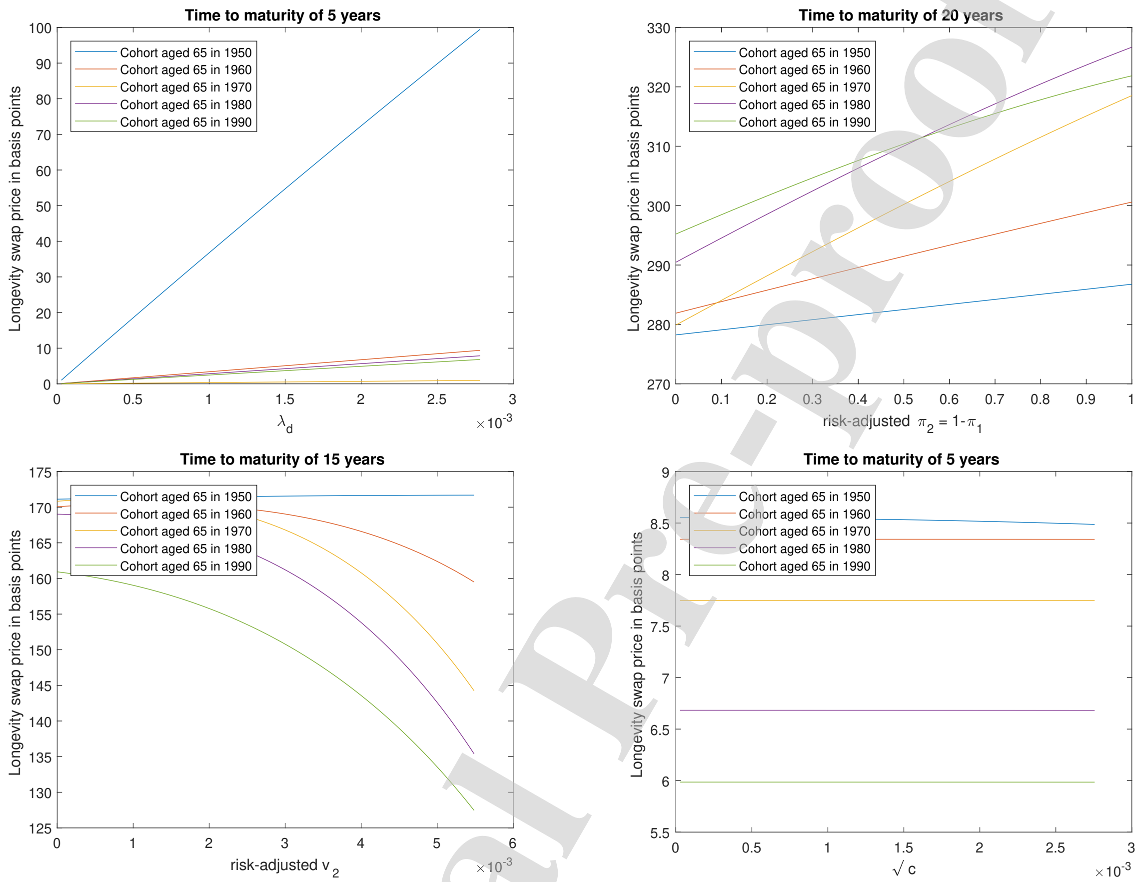

The top left plot shows the impact, for each cohort, on the price (in basis points) of a 5-year longevity swap when the parameter λ_d—measuring the market price of (diffusive) longevity risk—is changed from zero to $3\sqrt{c}$. The top right plot shows the impact, for each cohort, on the price (in basis points) of a 20-year longevity swap when the parameter $\bar{\pi}_2$—measuring the risk-neutral probability of a downward jump in mortality—is changed from zero to one. The bottom left plot shows the impact, for each cohort, on the price (in basis points) of a 15-year longevity swap when the parameter $\bar{v}_2$—measuring the inverse of the average absolute size of downward jumps—is changed from zero to three times its current size. The bottom right plot shows the impact, for each cohort, on the price (in basis points) of a 5-year longevity swap when the parameter $\sqrt{c}$—measuring the instantaneous (diffusive) volatility of the mortality intensity—is changed from (almost) zero to three times its current size.

Finally, and since Table 1 shows that the simpler OU process (with no jumps) can yield lower AIC and BIC statistics than our baseline model, Table 3 reports longevity swap prices for selected U.S. total population cohorts (aged 65) and maturities (in years), and for different values of the market price of longevity risk premium, under both setups. For all maturities and longevity risk premium values, the fair value of index-based survivor swaps has been declining for U.S. individuals completing the 65th anniversary in more recent decades. In relative terms, this decline is slightly more significant for shorter-term contracts than for longer arrangements. This is essentially explained by a general decline in mortality rates at all ages, particularly at older ages, with a switch from reducing premature deaths to extending the premature age range, by the rectangularization and compression of the survival curve under which life expectancy gains can only be generated by a decrease in lifespan variability (as evidenced by a small decline in the volatility coefficient of the mortality intensity) and by the progress in mean lifespan relative to progress in maximum lifespan.

The results in Table 3 for the five cohorts considered in this study show that, for all tenors and values of the market price of longevity risk, the longevity swap prices obtained using the baseline model are higher than those computed using the calibrated OU process. This suggests that the addition of the jump component to the random part of the stochastic process increases the survival rate of the population and, consequently, the longevity swap price. This is consistent with previous literature showing that higher randomness in the stochastic mortality intensity produces an improvement in the cohort survival probabilities—see, e.g., Luciano and Vigna (2008). Table 3 also shows that the longevity swap price difference between the two models is generally small, ranging between a minimum of 0.406% for the 5-year contract and a maximum of 14.238% for the 20-year swap, and increases with the maturity of the contract and the market price of longevity risk. The relative price differences are generally higher for younger cohorts when compared to older cohorts, with the exception being the cohort aged 65 years old in 1970 for which the differences are high. This result may be explained by the relatively weak fitting performance of the OU model in this cohort when compared to that of the Feller model and that obtained in other cohorts. Note also that the pricing solutions proposed are highly efficient: the 60 swap contracts are priced in only 0.06 seconds, under the baseline model, or 0.03 seconds, under the OU process.[14]

[14] Alternatively, solving the Riccati differential equation (45) through the fifth order *Runge-Kutta method* described in Press et al. (1994, Section 15.2), and computing the complex-valued function $\theta(t, T; \phi)$ by numerical integration of the ordinary differential equation (46)—using the (efficient) Gauss-Kronrod quadrature scheme provided by the *Matlab* built-in function "quadgk"—would yield a CPU time of 27.02 seconds for the whole set of 60 contracts (and under our baseline specification).

Table 3: Longevity swap prices for different U.S. cohorts.

Tenor (yrs)	k	Baseline model results for the cohort aged 65 in: 1950	1960	1970	1980	1990	OU results for the cohort aged 65 in: 1950	1960	1970	1980	1990
5 yrs	0.25	18.95	1.73	0.18	1.43	1.24	18.87	1.72	0.17	1.41	1.21
	0.50	37.79	3.46	0.35	2.85	2.47	37.63	3.43	0.35	2.81	2.43
	0.75	56.51	5.19	0.53	4.28	3.71	56.28	5.15	0.52	4.22	3.64
10 yrs	0.25	125.03	11.37	1.19	10.04	8.81	124.17	11.16	1.11	9.70	8.44
	0.50	248.84	22.73	2.37	20.06	17.61	247.18	22.36	2.26	19.44	16.93
	0.75	371.44	34.08	3.56	30.07	26.40	368.99	33.55	3.41	29.17	25.40
15 yrs	0.25	359.93	32.98	3.53	31.31	28.01	357.19	32.00	3.16	29.55	26.14
	0.50	716.09	65.93	7.07	62.58	55.99	710.82	64.17	6.54	59.31	52.50
	0.75	1068.45	98.84	10.60	93.81	83.93	1060.65	96.30	9.91	89.03	78.82
20 yrs	0.25	696.86	65.13	7.21	66.47	61.03	692.36	62.49	6.19	61.29	55.59
	0.50	1388.80	130.21	14.43	132.86	121.98	1380.22	125.46	12.93	123.23	111.86
	0.75	2075.51	195.25	21.64	199.18	182.85	2062.73	188.37	19.68	185.09	168.05
CPU time:		0.06 seconds					0.03 seconds				

This table shows longevity swap prices for selected U.S. total population cohorts and tenors (in years), under both the Feller with jumps (baseline) model and the OU process (without jumps), and for different values of the market price of longevity risk, which is defined as $\lambda_d = \frac{k}{\sqrt{c}}$. As in Table 2, the analysis is run using the model parameters specified in Table 1, a flat yield curve (with continuous compounding) at 2% per year, and strike prices K equal to the fitted survival schedule shown in Figure 1. All prices are expressed in basis points and as a percentage of the swap notional amount.

5. Conclusion

Traditional (Re)Insurance-based solutions for longevity risk management are expensive, entail significant bilateral counterparty credit risk exposure and are not an ultimate answer to the problem due to the undiversifiable nature of systematic longevity risk. The (re)insurance industry seems to be arriving to a point where natural hedging strategies are increasingly scarce and additional capacity to absorb longevity risk will only be possible by bringing in new capital and new investors from capital markets. As a result, in recent years, several capital-market-based solutions for mortality and longevity risk management have been proposed and, some, successfully launched. They comprise mortality- or longevity-linked debt instruments such as mortality and longevity bonds, and derivatives with both linear and nonlinear payoff structures, such as index-based longevity (or survivor) swaps, mortality and survivor options and survivor swaptions. A notable development in the market has been the issuance of longevity-linked structured notes incorporating derivative contracts (options), enabling coupon and/or redemption payments to depend on the performance of the underlying mortality or longevity index.

This paper is focused on the valuation of index-based capital-market longevity options and swaps using Fourier transforms. We apply a Fourier transform approach for European-style longevity option pricing under a continuous-time affine jump-diffusion model for both cohort mortality intensities and interest rates. Specifically, we propose a baseline model where the mortality intensity of a given cohort is driven by an affine jump-diffusion process featuring a non-mean reverting deterministic trend, a square-root diffusion component and a double exponential compound Poisson process, allowing for both (asymmetric) positive and negative mortality jumps of different sizes. We derive an analytic expression for the characteristic function of the underlying longevity index price process, obtain the Fourier transform of the dampened European longevity option price and compute the corresponding Fourier inversion to recover the option price via a Gauss-Lobatto quadrature scheme.

The affine jump-diffusion framework proposed in this paper is quite general and flexible and accommodates most short-rate and forward-rate mortality intensity models proposed in the literature. The valuation approach allows us to derive closed-from analytical expressions for the survival probability and for the characteristic function, and to price any longevity-linked security, such as q-forwards, S-forwards, longevity swaps, longevity options, endowments, longevity-linked life annuities, variable annuities and other structured contracts. The use of Fourier transforms for the valuation of longevity-linked options, which form the building blocks from which other more complex longevity-linked securities and derivatives can be constructed and priced, offers a new and efficient alternative to traditional pricing approaches such as the Black-Scholes-Merton framework, the martingale approach, tree-based methods and simulation-based approaches.

We describe in detail the model calibration approach and empirically investigate the fitting performance of five time-homogeneous affine jump diffusion specifications—including mean reverting and non-mean-reverting processes—using selected cohorts in the age range 65-100 from the U.S. total population (from 1950 to 2017). We provide empirical results on the valuation of index-based longevity swaps for different tenors and values of the market price of longevity risk premium. To gather further insight on the mortality model proposed, we investigate the sensitivity of longevity swap prices to changes in the baseline stochastic mortality model parameters and provide price results for an alternative model, the simpler Ornstein-Uhlenbeck process with no jumps.

The results obtained for the selected U.S. total population cohorts and tenors show that, for all maturities and longevity risk premium values, the fair value of index-based survivor swaps has been declining for U.S. individuals completing the 65th anniversary in more recent decades, particularly for shorter-term contracts. This is explained by a general decline in mortality rates at all ages observed during this period, by a switch in the composition of longevity improvements from reducing premature (younger ages) deaths to extending the premature age range, by the rectangularization and compression of the survival curve and by the progress in mean lifespan relative to progress in maximum lifespan. The results also show that for all tenors: (i) the longevity swap price increases with the market price of the diffusive longevity risk, with a more pronounced effect for older cohorts; (ii) the higher the risk-neutral probability of a negative jump in the mortality intensity and the higher its average size the more expensive longevity swap prices will be; (iii) the swap price is relatively insensitive to changes in the mortality intensity diffusive volatility; and (iv) the longevity swap prices obtained using the baseline Feller with jumps model are higher than those computed using the calibrated OU process for all cohorts, tenors and values of the market price of longevity risk considered in this study, suggesting that higher randomness in the stochastic mortality intensity produces an improvement in the cohort survival probabilities and, consequently, higher longevity swap prices.

Index-based longevity swaps and other capital market longevity-linked securities and derivatives offer pension schemes and annuity providers an efficient alternative to manage their longevity risk exposure but bring in bilateral counterparty credit risk to the extent that the risk cannot be partially or fully mitigated by collateralization. Further research is needed, under the Fourier transform valuation approach developed in this paper, to analyze and quantify the impact of bilateral credit risk on the marking-to-market of longevity swaps. The derivation and computation of the sensitivity measures (Greeks) that are required to perform dynamic hedging is also in the agenda for future research. Further investigation is also needed to assess the fitting and forecasting performance of alternative affine jump diffusion models considering different populations and cohorts.

References

Alonso-García, J., O. Wood and J. Ziveyi, 2018, Pricing and Hedging Guaranteed Minimum Withdrawal Benefits under a General Lévy Framework Using the COS Method, *Quantitative Finance* 18, 1049–1075.

Andersen, L. B. G. and V. V. Piterbarg, 2007, Moment Explosions in Stochastic Volatility Models, *Finance and Stochastics* 11, 29–50.

Ayuso, M., J. M. Bravo, and R. Holzmann, 2020, Getting Life Expectancy Estimates Right for Pension Policy: Period versus Cohort Approach, *Journal of Pension Economics and Finance*, 1–20. https://doi.org/10.1017/S1474747220000050.

Ballotta, L. and S. Haberman, 2006, The Fair Valuation Problem of Guaranteed Annuity Options: The Stochastic Mortality Environment Case, *Insurance: Mathematics and Economics* 38, 195–214.

Biffis, E., 2005, Affine Processes for Dynamic Mortality and Actuarial Valuations, *Insurance: Mathematics and Economics* 37, 443–468.

Biffis, E. and P. Millossovich, 2006, The Fair Value of Guaranteed Annuity Options, *Scandinavian Actuarial Journal* 19, 23–41.

Biffis, E., D. Blake, L. Pitotti, and A. Sun, 2016, The Cost of Counterparty Risk and Collateralization in Longevity Swaps, *Journal of Risk and Insurance* 83, 387–419.

Biffis, E., M. Denuit, and P. Devolder, 2010, Stochastic Mortality Under Measure Changes, *Scandinavian Actuarial Journal*, 284–311.

Biffis, E., Y. Lin, and A. Milidonis, 2017, The Cross-Section of Asia-Pacific Mortality Dynamics: Implications for Longevity Risk Sharing, *Journal of Risk and Insurance* 84, 515–532.

Björk, T., 1998, *Arbitrage Theory in Continuous Time* (Oxford University Press, New York).

Blake, D., A. J. G. Cairns, and K. Dowd, 2006, Living with Mortality: Longevity Bonds and Other Mortality-Linked Securities, *British Actuarial Journal* 12, 153–197.

Blake, D., A. J. G. Cairns, K. Dowd, and A.R. Kessler, 2019, Still Living with Mortality: The Longevity Risk Transfer Market After One Decade, *British Actuarial Journal* 24, 1–80.

Blake, D., A. J. G. Cairns, K. Dowd, and R. MacMin, 2006, Longevity Bonds: Financial Engineering Valuation and Hedging, *Journal of Risk and Insurance* 73, 647–672.

Blake, D. and W. Burrows, 2001, Survivor Bonds: Helping to Hedge Mortality Risk, *Journal of Risk and Insurance* 68, 339–348.

Boyer, M. and L. Stentoft, 2013, If We Can Simulate It, We Can Insure It: An Application to Longevity Risk Management, *Insurance: Mathematics and Economics* 52, 35–45.

Bravo, J. M., "Tábuas de Mortalidade Contemporâneas e Prospectivas: Modelos Estocásticos, Aplicações Actuariais e Cobertura Do Risco de Longevidade." PhD dissertation, Universidade de Évora 2007. Retrieved from: http://hdl.handle.net/10174/11148.

Bravo, J. M., 2011, Pricing Longevity Bonds Using Affine-Jump Diffusion Models, Working paper 2011/29, CEFAGE-UE.

Bravo, J. M., 2019, Funding for Longer Lives: Retirement Wallet and Risk-Sharing Annuities, *Ekonomiaz* 96, 268–291.

Bravo, J. M., 2020, Pricing Participating Longevity-Linked Life Annuities: A Bayesian Model Ensemble Approach, *Revised and resubmit to European Actuarial Journal.*

Bravo, J. M. and J. A. Herce, 2020, Career Breaks, Broken Pensions? Long-Run Effects of Early and Late-Career Unemployment Spells on Pension Entitlements, *Journal of Pension Economics and Finance*, 1–27. https://doi.org/10.1017/S1474747220000189.

Bravo, J. M. and N. El Mekkaoui de Freitas, 2018, Valuation of Longevity-Linked Life Annuities, *Insurance: Mathematics and Economics* 78, 212–229.

Bravo, J. M., M. Ayuso, R. Holzmann, and E. Palmer, 2020, Addressing the Life Expectancy Gap in Pension Policy, *Revised and resubmit to Insurance: Mathematics and Economics.*

Cairns, A. J. G. and G. El Boukfaoui, 2019, Basis Risk in Index-Based Longevity Hedges: A Guide for Longevity Hedgers, *North American Actuarial Journal*, 1–22. doi:10.1080/10920277.2019.1651658.

Cairns, A. J. G., D. Blake, and K. Dowd, 2006a, Pricing Death: Framework for the Valuation and Securitization of Mortality Risk, *ASTIN Bulletin* 36, 79–120.

Cairns, A. J. G., D. Blake, and K. Dowd, 2006b, A Two-Factor Model for Stochastic Mortality with Parameter Uncertainty: Theory and Calibration, *Journal of Risk and Insurance* 73, 687–718.

Cairns, A. J. G, D. Blake, and K. Dowd, 2008, Modelling and Management of Mortality Risk: A Review, *Scandinavian Actuarial Journal*, 79–113.

Carr, P. and D. Madan, 1999, Option Valuation Using the Fast Fourier Transform, *Journal of Computational Finance* 2, 61–73.

Chan, W.S., J.S.-H. Li, and J. Li, 2014, The CBD Mortality Indexes: Modeling and Applications, *North American Actuarial Journal* 18, 38–58.

Chang, C., C. Chen, and M. H. Tsay, 2010, Pricing Survivor Swaps with Mortality Jumps and Default Risk, *Academia Economic Papers* 38, 119–156.

Chau, K. W., S. C. P. Yam, and H. Yang, 2015, Fourier-Cosine Method for Gerber-Shiu Functions, *Insurance: Mathematics and Economics* 61, 170–180.

Cont, R. and P. Tankov, 2004, *Financial Modelling with Jump Processes* (Chapman and Hall/CRC, London).

Coughlan, G.D., D. Epstein, A. Sinha, and P. Honig, 2007, Q-Forwards: Derivatives for Transferring Longevity and Mortality Risks, Working paper, J. P. Morgan Pension Advisory Group, London.

Cox, J., J. Ingersoll, and S. Ross, 1985, A Theory of the Term Structure of Interest Rates, *Econometrica* 53, 385–407.

Cox, S.H., Y. Lin, and S. Wang, 2006, Multivariate Exponential Tilting and Pricing Implications for Mortality Securitization, *Journal of Risk and Insurance* 73, 719–736.

Cui, J., 2008, Longevity Risk Pricing, Netspar discussion paper, dp 2008-001.

Dahl, M., 2004, Stochastic Mortality in Life Insurance: Market Reserves and Mortality-Linked Insurance Contracts, *Insurance: Mathematics and Economics* 35, 113–136.

Dahl, M., M. Melchior, and T. Møller, 2008, On Systematic Mortality Risk and Risk-Minimization with Survivor Swaps, *Scandinavian Actuarial Journal*, 114–146.

Dahl, M., S. Glar, and T. Møller, 2011, Mixed Dynamic and Static Risk-Minimization with an Application to Survivor Swaps, *European Actuarial Journal* 1, 233–260.

D'Amato, V., E. Di Lorenzo, S. Haberman, P. Sagoo, and M. Sibillo, 2018, De-Risking Strategy: Longevity Spread Buy-in, *Insurance: Mathematics and Economics* 79, 124–136.

Davis, R., 1973, Numerical Inversion of a Characteristic Function, *Biometrika* 60, 415–417.

Dawson, P., K. Dowd, A.J.G. Cairns, and D. Blake, 2010, Survivor Derivatives: A Consistent Pricing Framework, *Journal of Risk and Insurance* 77, 579–596.

Dawson, P., K. Dowd, D. Blake, and A. J. G. Cairns, 2009, Options on Normal Underlyings with An Application to the Pricing of Survivor Swaptions, *Journal of Futures Markets* 29, 757–774.

Dowd, K., 2003, Survivor Bonds: A Comment on Blake and Burrows, *Journal of Risk and Insurance* 70, 339–348.

Dowd, K., D. Blake, A. J. G. Cairns, and P. Dawson, 2006, Survivor Swaps, *Journal of Risk and Insurance* 73, 1–17.

Duffie, D., J. Pan, and K. Singleton, 2000, Transform Analysis and Asset Pricing for Affine Jump-Diffusions, *Econometrica* 68, 1343–1376.

Friedberg, L. and A. Webb, 2005, Life is Cheap: Using Mortality Bonds to Hedge Aggregate Mortality Risk, CRR working paper 2005-13.

Fung, M. C., K. Ignatieva, and M. Sherris, 2019, Managing Mortality Risk in Life Annuities: An Application of Longevity Derivatives, *Risks, MDPI, Open Access Journal* 7, 1–25.

Gander, W. and W. Gautschi, 2000, Adaptive Quadrature - Revisited, *BIT* 40, 84–101.

Heath, D., R. Jarrow, and A. Morton, 1992, Bond Pricing and the Term Structure of Interest Rates: A New Methodology for Contingent Claims Valuation, *Econometrica* 60, 77–105.

Human Mortality Database, 2019, University of California, Berkeley (USA), and Max Planck Institute for Demographic Research (Germany), Available at www.mortality.org or www.humanmortality.de (data downloaded on [15-August-2019]).

Hunt, A. and D. Blake, 2015, Modelling Longevity Bonds: Analysing the Swiss Re Kortis Bond, *Insurance: Mathematics and Economics* 63, 12–29.

Kahl, C. and P. Jäckel, 2005, Not-so-Complex Logarithms in the Heston Model, *Wilmott Magazine* 19, 94–103.

Kou, S. G. and H. Wang, 2004, Option Pricing under a Double Exponential Jump Diffusion Model, *Management Science* 50, 1178–1192.

Lamberton, D. and B. Lapeyre, 1996, *Introduction to Stochastic Calculus Applied to Finance* (Chapman & Hall/CRC, London).

Lee, R., 2004, Option Pricing by Transform Methods: Extensions, Unification, and Error Control, *Journal of Computational Finance* 7, 51–86.

Lee, R. and L. Carter, 1992, Modelling and Forecasting the Time Series of US Mortality, *Journal of the American Statistical Association* 87, 659–671.

Levantesi, S. and M. Menzietti, 2006, Maximum Market Price of Longevity Risk under Solvency Regimes: The Case of Solvency II, *Risks, MDPI, Open Access Journal* 5, 1–21.

Li, J. S., J. Li, U. Balasooriya, and K. Zhou, 2019, Constructing Out-of-the-Money Longevity Hedges Using Parametric Mortality Indexes, *North American Actuarial Journal*, 1–32.

Li, Y. and J. S. Liu, 2015, The Age Pattern of Transitory Mortality Jumps and its Impact on the Pricing of Catastrophic Mortality Bonds, *Insurance: Mathematics and Economics* 64, 135–150.

Lin, Y. and S. H. Cox, 2005, Securitization of Mortality Risks in Life Annuities, *Journal of Risk and Insurance* 72, 227–252.

Lin, Y. and S. H. Cox, 2007, Longevity Risk, Rare Event Premia and Securitization, Working paper, University of Nebraska - Lincoln and University of Manitoba.

Lin, Y., S. H. Cox, and H. Pedersen, 2010, Mortality Risk Modeling: Applications to Insurance Securitization, *Insurance: Mathematics and Economics* 46, 242–253.

LLMA, 2010, Technical note: The s-forward. London: Life and longevity markets association (LLMA).

Lord, R. and C. Kahl, 2007, Optimal Fourier Inversion in Semi-Analytical Option Pricing, *Journal of Computational Finance* 10, 1–30.

Luciano, E. and E. Vigna, 2008, Mortality Risk Via Affine Stochastic Intensities: Calibration and Empirical Relevance, *Belgian Actuarial Journal* 8, 5–16.

Luciano, E., L. Regis, and E. Vigna, 2012, Delta-Gamma Hedging of Mortality and Interest Rate Risk, *Insurance: Mathematics and Economics* 50, 402–412.

Michaelson, A. and J. Mulholland, 2014, Strategy for Increasing the Global Capacity for Longevity Risk Transfer: Developing Transactions That Attract Capital Markets Investors, *Journal of Alternative Investments* 17, 18–27.

Michaelson, A. and J. Mulholland, 2015, Strategy for Increasing the Global Capacity for Longevity Risk Transfer, in B.R. Bruce, ed.: *Pension and Longevity Risk Transfer for Institutional Investors* (Institutional Investor Journals), 28–37.

Milevsky, M. and S. Promislow, 2001, Mortality Derivatives and the Option to Annuitise, *Insurance: Mathematics and Economics* 29, 299–318.

Milevsky, M., S. D. Promislow, and V. R. Young, 2005, Financial Valuation of Mortality Risk Via the Instantaneous Sharpe Ratio: Applications to Pricing Pure Endowments, Working paper. Ann Arbor: University of Michigan. Available at: http://arxiv.org/ abs/0705.1302.

Miltersen, C. and S. A. Persson, 2006, Is Mortality Dead? Stochastic Forward Force of Mortality Rate Determined by No Arbitrage, Working paper, Norwegian School of Economics and Business Administration.

Nunes, J., 2004, Multifactor Valuation of Floating Range Notes, *Mathematical Finance* 14, 79–97.

Nunes, J. and T. Alcaria, 2016, Valuation of Forward Start Options under Affine Jump-Diffusion Models, *Quantitative Finance* 16, 727–747.

Press, W., B. Flannery, S. Teukolsky, and W. Vetterling, 1994, *Numerical Recipes in Pascal: The Art of Scientific Computing* (Cambridge University Press, Cambridge).

Sánchez-Romero, M., R. Lee, and A. Prskawetz, 2020, Redistributive Effects of Different Pension Systems When Longevity Varies by Socioeconomic Status, *The Journal of the Economics of Ageing* 17, https://doi.org/10.1016/j.jeoa.2020.100259.

Schräger, D., 2006, Affine Stochastic Mortality, *Insurance: Mathematics and Economics* 35, 81–97.

Vasiček, O., 1977, An Equilibrium Characterization of the Term Structure, *Journal of Financial Economics* 5, 177–188.

Wang, C. and S. Yang, 2013, Pricing Survivor Derivatives with Cohort Mortality Dependence under the Lee-Carter Framework, *Journal of Risk and Insurance* 80, 1027–1056.

Wang, S., 2002, A Universal Framework for Pricing Financial and Insurance Risks, *ASTIN Bulletin* 32, 213–234.

Yueh, M.-L., H.-Y. Chiu, and S.-H. Tsai, 2016, Valuations of Mortality-Linked Structured Products, *Journal of Derivatives* 24, 66–87.

Zeddouk, F. and P. Devolder, 2019, Pricing of Longevity Derivatives and Cost of Capital, *Risks, MDPI, Open Access Journal* 7, 1–29.

Zhu, N. and D. Bauer, 2011, Applications of Forward Mortality Factor Models in Life Insurance Practice, *The Geneva Papers on Risk and Insurance – Issues and Practice* 36, 567–594.